



Article

# Optimal Design of Reverse Logistics Recycling Network for Express Packaging Considering Carbon Emissions

Jia Mao <sup>1</sup>, Jinyuan Cheng <sup>1</sup>, Xiangyu Li <sup>1</sup>, Honggang Zhao <sup>2,\*</sup>  and Ciyun Lin <sup>1</sup> <sup>1</sup> School of Transportation, Jilin University, Changchun 130022, China<sup>2</sup> College of Chemical Engineering, Xinjiang Normal University, Urumqi 830054, China

\* Correspondence: 107621997010002@xjnu.edu.cn

**Abstract:** With the development of China's express delivery industry, the number of express packaging has proliferated, leading to many problems such as environmental pollution and resource waste. In this paper, the process of reverse logistics network design for express packaging recycling is given as an example in the M region, and a four-level network containing primary recycling nodes, recycling centers, processing centers, and terminals is established. A candidate node selection model based on the K-means algorithm is constructed to cluster by distance from 535 courier outlets to select 15 candidate nodes of recycling centers and processing centers. A node selection model based on the NSGA-II algorithm is constructed to identify recycling centers and processing centers from 15 candidate nodes with minimizing total cost and carbon emission as the objective function, and a set of Pareto solution sets containing 43 solutions is obtained. According to the distribution of the solution set, the 43 solutions are classified into I, II, and III categories. The results indicate that the solutions corresponding to Class I and Class II solutions can be selected when the recycling system gives priority to cost, Class II and Class III solutions can be selected when the recycling system gives priority to environmental benefits, and Class III solutions can be selected when the society-wide recycling system has developed to a certain extent. In addition, this paper also randomly selects a sample solution from each of the three types of solution sets, conducts coding interpretation for site selection, vehicle selection, and treatment technology selection, and gives an example design scheme.



**Citation:** Mao, J.; Cheng, J.; Li, X.; Zhao, H.; Lin, C. Optimal Design of Reverse Logistics Recycling Network for Express Packaging Considering Carbon Emissions. *Mathematics* **2023**, *11*, 812. <https://doi.org/10.3390/math11040812>

Academic Editor: Yaping Ren

Received: 11 January 2023

Revised: 29 January 2023

Accepted: 3 February 2023

Published: 5 February 2023



**Copyright:** © 2023 by the authors. Licensee MDPI, Basel, Switzerland. This article is an open access article distributed under the terms and conditions of the Creative Commons Attribution (CC BY) license (<https://creativecommons.org/licenses/by/4.0/>).

**Keywords:** express packaging; green reverse logistics; reduce carbon emissions; K-means algorithm; bi-objective model; NSGA-II algorithm

**MSC:** 93-10

## 1. Introduction

In recent years, to promote the high-quality development of green couriers, green transportation, green consumption, and other areas, the concept of saving has been deeply rooted in people's hearts; green low-carbon mode of production and lifestyle is accelerating the formation. The report of the 20th National Congress of the Communist Party of China proposed to "accelerate the green transformation of the development mode", and such measures are especially evident in the express delivery industry. The 2021 government work report clearly pointed out that we should strengthen the construction of urban and rural circulation systems, especially to speed up e-commerce and express into the countryside, and expand consumption at the county and township level, which is the eighth time "express" was included in the government work report. According to the National Bureau of Statistics data, China's 2011–2021 express business volume increased significantly (see Figure 1). At the same time, along with the in-depth implementation of the new development pattern strategy, China's express industry will certainly enter a new stage of development shortly, bringing a new round of growth in the volume of express business and its revenue [1–4].

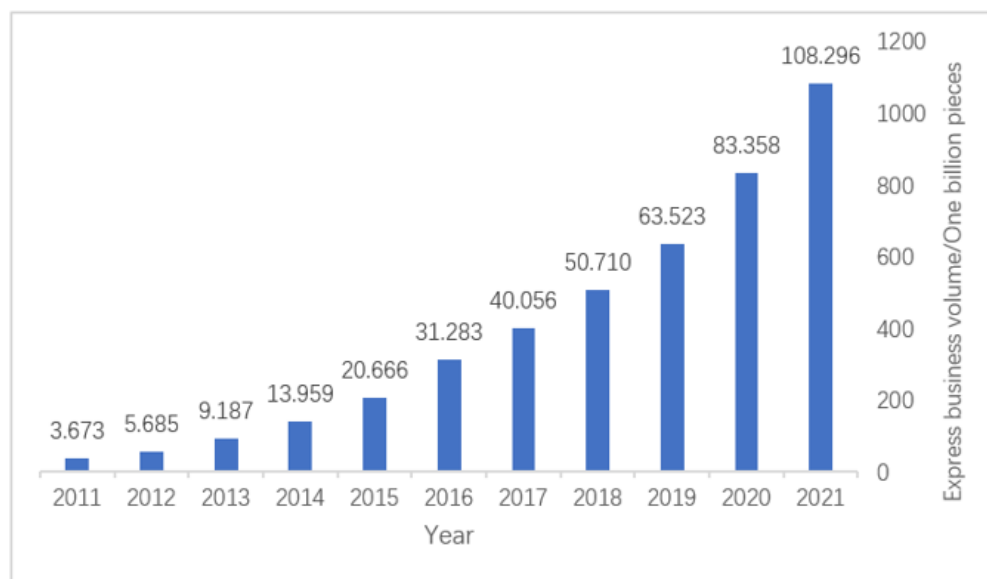


**Figure 1.** The 2011–2021 express business volume.

The monitoring data of the State Post Bureau showed that the country received 569 million express parcels on the Double Eleven, an increase of 28.54% year-on-year. However, the rapid development of the express industry has also brought about many social and environmental problems; especially the environmental pollution, management chaos, and waste of resources caused by express packaging waste are increasingly obvious [5–7]. Data show that in China’s megacities, the increment of express packaging waste has accounted for 93% of the increment of domestic waste, and in some large cities 85% to 90%. How to effectively manage courier waste has become an urgent environmental problem to be solved. The main problems are manifested in the following areas.

- (1) The phenomenon of excessive packaging of express products. The problem is more common in the current courier industry because the first impression of consumers on the courier packaging directly affects the entire shopping experience, and the contribution of consumer shopping satisfaction is greater, so e-commerce merchants in the delivery of goods based on basic protective protection, usually increase the protective measures to avoid damage and other situations in transit [8–10].
- (2) Some of the courier packaging used in the production of materials with poor environmental performance, resulting in packaging waste that is difficult to naturally degrade. The common airbag foam padding, tape, and black bags made of PVC and other materials in courier packaging degrade slowly under natural conditions and produce a lot of toxic and harmful substances when incinerated [11].
- (3) The existing courier packaging has a low degree of standardization and a low reuse rate. The development of express packaging standards involves many aspects, such as packaging materials, filler materials, size specifications, plastic sealing methods, marking, and inspection methods. Low standardization will, on the one hand, reduce logistics efficiency, reduce the management level and quality of logistics services, and increase unnecessary costs, and on the other hand, reduce packaging mobility, narrow the scope of application, increase the difficulty of coordinating the use of express packaging, and make the overall recycling rate lower [12].
- (4) The overall recycling rate of express packaging is low. A related research study shows that the actual recycling rate of cardboard and recyclable plastic in China in a year is less than 10%, and the overall courier packaging recycling rate is less than 20%. In some densely populated cities, the incremental amount of courier packaging waste accounts for more than 90% of the total incremental amount of domestic waste.

- (5) The reverse logistics system of express packaging recycling is not sound, and systematic scientific planning guidance is missing, manifested by the lagging work of express packaging classification, the confusion of social recycling channels and the low degree of specialization of treatment methods, the inadequacy of institutional mechanisms of relevant enterprises and government departments, the lack of laws and regulations and policy support, and the low enthusiasm of consumer participation in recycling [13–16].

Promoting the green transformation of express packaging, solving the bottlenecks faced by the industry, and achieving the sustainable development of the express industry is a complex and long-term systemic project that requires the participation and joint efforts of experts from different fields and different industry sectors [17]. In response to the above-mentioned problems in the express delivery industry, scholars have studied express packaging recycling from different perspectives.

In terms of site selection, Harsaj proposed a fuzzy multi-objective optimization model that quantifies three aspects simultaneously: economic, environmental, and social, and solved it using an improved particle swarm algorithm (PSO), and finally validated the model with a medical syringe recycling system [18]. Gao proposed a reverse logistics network design scheme based on a forward logistics network, and constructed an optimization model based on a multi-objective scenario with the objective functions of maximizing the expected total monetary profit, minimizing the expected total carbon emission cost, and maximizing the expected total job creation, and transformed it into a single-objective model to finally obtain the Pareto-optimal solution, and finally validated the effectiveness by using tires as an example [19]. Nie studied the supply chain configuration problem, constructed a mixed integer linear programming model with minimizing carbon emissions as the objective function, solved it using dynamic programming algorithms, and finally carried out an example verification to achieve a balance between economic and social benefits [20]. Guo studied fresh food distribution, built a two-stage model, considered the total system cost and vehicle path, and solved using a genetic algorithm and particle swarm algorithm, which effectively reduced carbon emissions and total cost [21]. Reddy constructed a multi-level multi-period mixed integer linear programming model with profit maximization as the objective function, considering the effects of facility location, vehicle type, and return rate, and finally gave an example analysis [22].

From the perspective of recycling model selection research, Liang used the Internet as a bridge to realize the design of a virtual APP and recycling device from the perspective of consumer psychology, real consumption situation, and the current situation of packaging recycling, to form a complete express packaging recycling system [2]. Yang constructed a multi-agent express packaging waste recycling system including the government, individuals, and enterprises. Based on differential game theory, the behavioral characteristics of individuals and the optimal strategies of government and enterprises under the market-driven recycling model, government-driven recycling model, and cooperative-driven recycling model were explored [23]. Based on previous studies by scholars, the main research contributions of this paper are as follows [24].

- From the concept of reducing carbon emission and environmental pollution, this paper gives the process of designing the reverse logistics network for express packaging recycling, taking the M region as an example, and establishes a four-level network containing primary recycling nodes, recycling centers, processing centers, and terminals.
- Construct a candidate node selection model based on the K-means algorithm, cluster by distance from 535 express outlets, and use the obtained basic data to calculate the distance between each node, the express volume of each node, etc.
- Construct a node selection model based on the NSGA-II algorithm, with the objective function of minimizing the total cost and carbon emission, and consider the effects of different locations of the selected nodes, different types of vehicles between nodes, and different processing technologies adopted by the processing centers.

## 2. Problem Description

In this paper, according to the economic development and administrative division of Changchun, seven district administrative units under Changchun are selected as the area under study (hereinafter collectively referred to as M area), including Nangan District, Kuancheng District, Chaoyang District, Erdao District, Lvyuan District, Shuangyang District, and Jiutai District (not considering Gongzhuling District). In this paper, we design the reverse logistics network for express packaging in region M. The regional map of region M is shown in Figure 2.

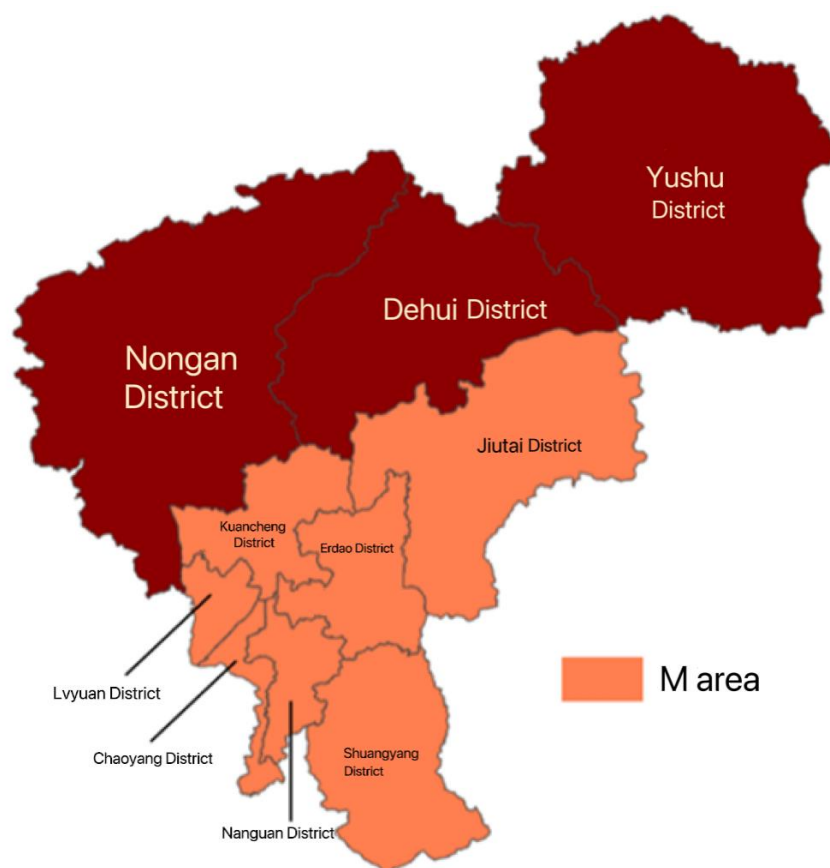


**Figure 2.** Regional map of M area.

According to the relevant data from Changchun Bureau of Statistics, this paper obtains the 2018–2020 population figures for the seven administrative regions mentioned above, as shown in Appendix A Table A1.

The proportion of the population of each district to the total population of Changchun was obtained (see Appendix A Table A2), in which the average proportion of the municipal districts to the total population of the city from 2018 to 2020 was the weighted average, and the weights of each year from 2018 to 2020 were 0.5, 0.3, and 0.2 according to the principle that the closer the year, the greater the weight.

In this paper, Baidu map API was used to obtain the original data of the latitude and longitude of courier points in the M area of Changchun and obtain 535 final valid data points after eliminating individual invalid data points, including 99 in Nangan District, 81 in Kuancheng District, 107 in Chaoyang District, 103 in Erdao District, 81 in Lvyuan District, 17 in Shuangyang District, and 47 in Jiutai District. The latitude and longitude of express points in Nangan District are shown in Appendix A Table A3, and the rest of the areas are omitted.

The relevant statistical information of Changchun Postal Administration was checked to obtain the express business volume in Changchun from 2013 to 2020, as shown in Table 1.

**Table 1.** The 2013–2020 express business statistics table in Changchun.

Year	Express Business Volume/Million Pieces	Year	Express Business Volume/Million Pieces
2013	27.1409	2017	98.9954
2014	41.3411	2018	129.7255
2015	52.3329	2019	161.9971
2016	78.6633	2020	237.2633

To meet the design requirements of the subsequent recycling network, the data in Table 1 need to be used to forecast the express business volume of Changchun in the next few years and select the appropriate value as the design value. In this paper, the least squares method is used to fit a linear function and an exponential function to the express business volume data of Changchun from 2013 to 2020, and the obtained functional relationships are shown in Equations (1) and (2).

$$y = 2242.9x - 540.05 \tag{1}$$

$$y = 2183e^{0.2971x} \tag{2}$$

In the above Equations (1) and (2),  $x = Year - 2012$ . The fitted image is shown in Figure 3, and it can be visually seen that the fitting effect of Equation (2) is better than the fitting effect of Equation (1). Using Equations (1) and (2), the prediction of express business volume for 2013–2020 and 2021–2025 is shown in Table 2 and Figure 3.

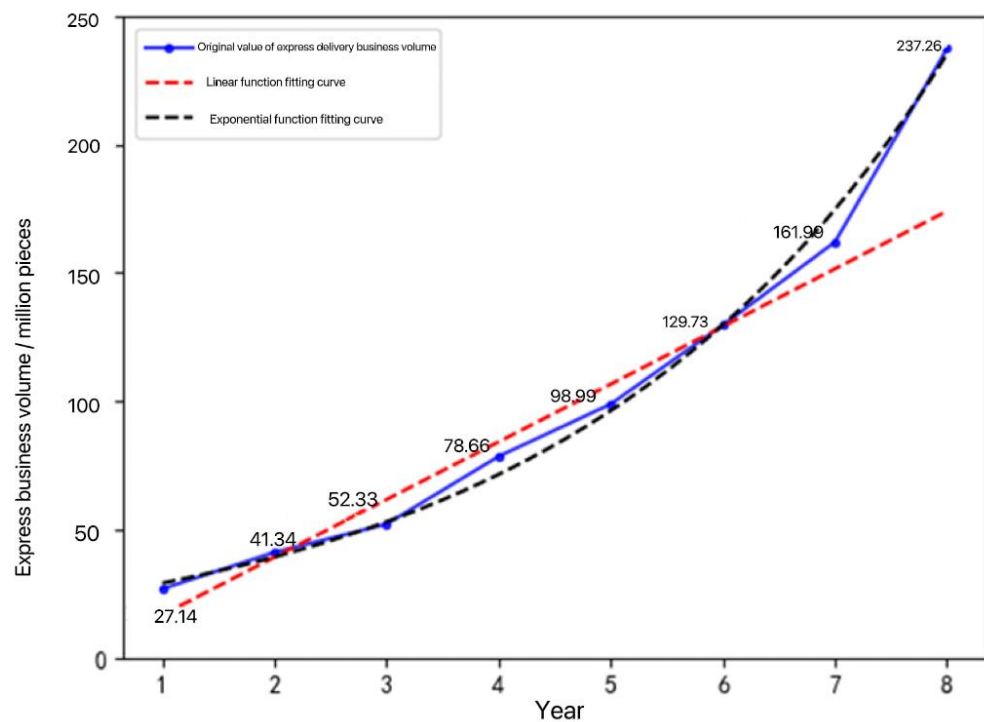


**Figure 3.** Fitting graph of express business volume.

**Table 2.** Express business volume forecast.

Serial Number	Actual Value/ Million Pieces	Linear Forecast Value/Million Pieces	Error	Index Forecast Value/Million Pieces	Error
1	27.1409	17.0285	37.26%	29.38209	8.26%
2	41.3411	39.4575	4.56%	39.54682	4.34%
3	52.3329	61.8865	18.26%	53.22803	1.71%
4	78.6633	84.3155	7.19%	71.64226	8.93%
5	98.9954	106.7445	7.83%	96.4269	2.59%
6	129.7255	129.1735	0.43%	129.7858	0.05%
7	161.9971	151.6025	6.42%	174.6851	7.83%
8	237.2633	174.0315	26.65%	23511.74	0.90%
9	/	196.4605	/	316.4563	/
10	/	218.8895	/	425.9343	/
11	/	241.3185	/	573.2863	/
12	/	263.7475	/	771.6146	/
13	/	286.1765	/	1038.555	/

As we can see in Table 3, the prediction effect of Equation (2) is better than that of Equation (1), so the express volume of 103,855,000 pieces in 2025 (x = 13) predicted by Equation (2) is selected as the design value.

**Table 3.** The parameters given in this paper and their values.

$M = 6000 \text{ kg}$	$c = 4000 \text{ kg/m}^2$
$m_0 = 0.3 \text{ kg}$	$c_{ar1} = 0.00800 \text{ kg/m}^2$
$V_{max} = 30,000,000 \text{ pieces}$	$c_{ar2} = 0.00804 \text{ kg/m}^2$
$V_{max}m_0 = 9,000,000 \text{ kg}$	$c_{ar3} = 0.00808 \text{ kg/m}^2$
$C_1 = 1200 \text{ CNY/m}^2$	$a_1 = 1.2500 \text{ CNY/kg}$
$C_2 = 900 \text{ CNY/m}^2$	$a_2 = 1.2400 \text{ CNY/kg}$
$C_3 = 850 \text{ CNY/m}^2$	$a_3 = 1.2300 \text{ CNY/kg}$
$C_4 = 800 \text{ CNY/m}^2$	$\alpha = 0.5, \beta = 0.2, \gamma = 0.3$

### 3. Algorithm Introduction

#### 3.1. Introduction to K-Means Algorithm

##### 3.1.1. Principle of K-Means Algorithm

The K-means algorithm belongs to unsupervised machine learning and is a common classical clustering algorithm with the advantages of simplicity, efficiency, and ease of implementation, but it is sensitive to the selection of the initial clustering centers, which can affect the accuracy and speed of convergence if not selected properly. The K-means problem in a general sense can be described as follows: given a dataset containing N elements, each of which is an M-dimensional real vector, the objective is to select K points as clustering centers and divide the N elements into K sets, where each set corresponds to a clustering center so that the sum of the squared distances of all elements to the corresponding clustering center is minimized, at which point the clustering center of each set is the mean point of each set element [25].

##### 3.1.2. K Value Determination Method

- (1) Select-on-demand method: This means that the number of classification groups of data is determined according to the actual demand.
- (2) Elbow method: error squared and SSE is a function of the number of clusters K, SSE becomes smaller with the increase of K, and when K increases to a certain value, the rate of change of SSE will rapidly become smaller; that is, as the value of K continues to increase and tends to level off, so that the relationship between K and SSE graph is similar to the elbow, the inflection point of the elbow is the optimal number of clusters K.

- (3) Contour coefficient method: the contour coefficient of a certain data point of a cluster is the difference between the average distance (cohesion) of the data and the data of the same cluster and the average distance (separation) of all data of the nearest cluster and the ratio of the larger of the two. After finding the data, the contour coefficient of the rest of the data in the same cluster is obtained, and the average value is the average contour coefficient of the data in the group. The larger the average contour coefficient, the better the clustering effect, the corresponding K value is the optimal number of clusters.
- (4) Gap Statistics method: in the sample area in accordance with the uniform distribution of randomly generated and the original sample number of random samples, and these random samples and K-means clustering, calculate the loss of random samples and the actual sample loss of the difference between the maximum value of the corresponding K is the optimal number of clusters.

### 3.2. Introduction of NSGA-II Algorithm

#### 3.2.1. Introduction to Multi-Objective Optimization Algorithms

When there are two or more objective functions, it is called multi-objective optimization.

The general form of multi-objective optimization is shown in Equation (3).

$$\min F = [f_1(x), f_2(x), f_3(x), \dots, f_m(x)]^T \quad (3)$$

In the above equation,  $F(x)$  is the multi-objective optimization result,  $f_1(x), f_2(x), f_3(x), \dots, f_m(x)$  is the objective component, and  $m$  is the objective dimension.

#### 3.2.2. Introduction to NSGA-II Algorithm

NSGA-II algorithm is a commonly used multi-objective genetic algorithm with the advantages of lower computational complexity and better population goodness and diversity. Its core is the introduction of fast non-dominated sorting, crowding degree, and elite strategy, as shown below [26].

- (1) Introduction to the fast non-dominated sorting method.

Let  $n_i$  denote the number of individuals dominating individual  $i$  in the population, and  $S_i$  is the set of individuals dominated by individual  $i$ . Find all individuals with  $n_i = 0$  in the population, i.e., the number of individuals dominating individual  $i$  is 0, i.e., individual  $i$  is not dominated, and deposit the eligible individual  $i$  into the non-dominated set R1, which means the subdominated rank is 1.

For all individuals  $j$  in the current non-dominated set R1, iterate through the set  $S_j$  of the individuals it dominates. Since the individuals  $j$  dominating individual  $t$  have been deposited in the current non-dominated set R1, the  $n_t$  of each individual  $t$  in the set  $S_j$  is subtracted by 1. That is, the number of individuals governing the solution of individual  $t$  is reduced by 1. If  $n_t - 1 = 0$  is satisfied, then individual  $t$  is deposited in the set H.

R1 is used as the first level of the set of non-dominated individuals, and the individuals in this set are only dominated by other individuals and not by any other individuals, and all individuals in this set are assigned the same non-dominated ranking level, and then the above grading operation is continued for the set H, and the corresponding ranking level is also assigned, until all individuals are graded, i.e., all individuals are assigned the corresponding ranking level.

- (2) Crowding degree profile.

The crowding degree  $i_d$  denotes the density of individuals around a given point in a population of a given generation, and in practice, it is measured by the length of the largest rectangle around individual  $i$  that contains individual  $i$  but not other individuals, where the crowding degree of individuals on each rank boundary is  $+\infty$ . According to the definition

of crowding degree, it can be seen that the larger the crowding degree is, the better the individuals are. The specific algorithm text is not repeated.

(3) Introduction to the elite strategy.

The elite strategy is to prevent the elimination of good individuals in the population in each generation, and to mix all individuals in the parent and child generations, and then select them according to the rank of non-dominance sorting and the size of crowding degree to get the new generation population that meets the population size requirement, effectively avoiding the loss of good individuals in the parent population, and the execution process is shown in Figure 4 [27].

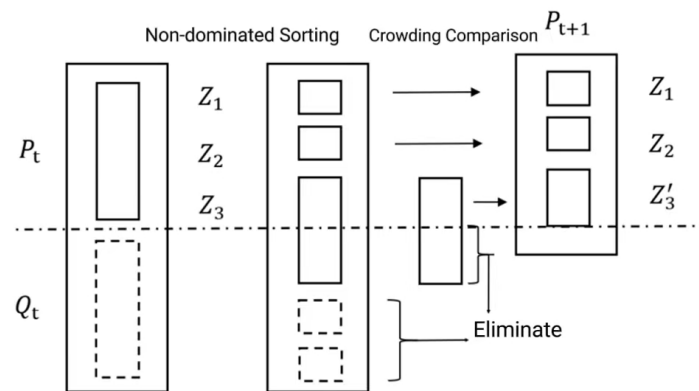


Figure 4. Elite strategy diagram.

As shown above, firstly, the parents  $P_t$  and  $Q_t$  are merged to obtain a new population with two times the original population size, and the individuals in the new population are sorted non-dominantly and selected according to the rank of non-dominant rank from smallest to largest until the selection reaches the rank of  $Z_i$ , so that the number of selected individuals plus the number of individuals in this rank is greater than the original population size for the first time, and then the  $Z_i$  is calculated.  $Z_i$  rank in the crowding degree of individuals, and according to the size of the crowding degree from the largest to the smallest selection, until the population number requirement is met, so that the new generation of parents  $P'_t$ .

#### 4. Model Building

##### 4.1. Modeling of Reverse Logistics Network in M Region

This paper determines the third-party logistics-centered express packaging model considering government participation, i.e., in the subsequent design of this paper, it is assumed that a third-party logistics enterprise specializing in express packaging recycling will carry out unified recycling and processing of express packaging of each courier company.

##### 4.1.1. Network Level and Node Analysis

According to the development status of the M region, this paper designs a four-layer recycling network, and the schematic diagram of express packaging reverse logistics network layers and nodes in the M region is shown in Figure 5.

Among them, the first level is the primary recycling layer; the nodes of this level are the 535 courier points acquired, responsible for the recovery of express packaging directly from consumers, mainly by the consumers themselves to return express packaging, supplemented by door-to-door service for recycling. The second level is the recycling level; the node of this level is the recycling center, which is responsible for collecting and storing the express packaging recovered by the courier points within a certain area and connects to the primary recycling level with the relevant carriers leased or purchased, and the transportation process is short-distance transportation. The third level is the processing layer; the node of this level is the processing center, which is responsible for classifying the



express packaging recovered by each recycling center and carrying out different technical treatments according to different categories, mainly including reuse treatment and transport to each recycling center, transport to the paper mill, and transport to landfill, with the relevant carrier leased or purchased to connect the recycling layer and the terminal layer, the transport process is medium and long-distance transport compared with the transport process of the first and second levels. The transportation process is medium to long distance compared to the first and second levels. The fourth level is the terminal level, the nodes of this level are the paper mill and the landfill, which are responsible for accepting the express packaging after sorting in the processing center, the longitude and latitude of the paper mill and the landfill are (43.910551° N, 125.420776° E) and (43.964575° N, 125.358692° E), and they are connected to the processing level by the relevant carriers leased or purchased. The process is also medium to long distance.

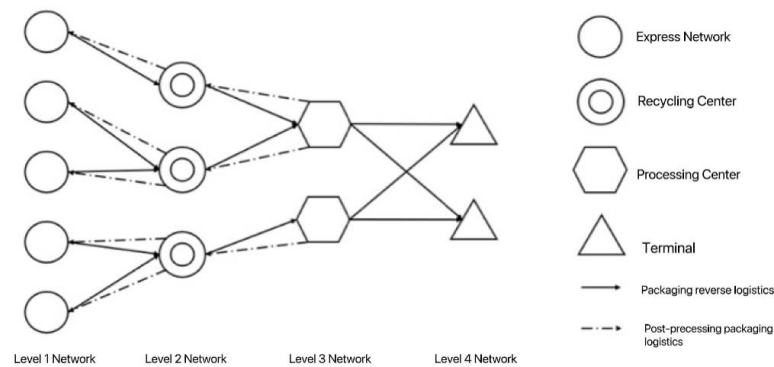


**Figure 5.** Schematic diagram of express packaging reverse logistics network hierarchy and nodes in M region.

4.1.2. Determination of Candidate nodes Based on the K-Means Algorithm

- Basic assumptions

(1) Euclidean distance is used in this paper to calculate the distance between the data and the center of clusters (center of mass).

(2) It is assumed that the influence of the Earth’s surface on the distance calculation is negligible in the range of M region.

- Symbol Description

Symbols	Meaning
$SSE$	Clustering error of all sample data.
$V$	New cluster center and old cluster center error.
$K$	Number of cluster centers $K_i$ set of values, $K = \{1, 2, \dots, N - 1, N\}$ .
$K_0$	Number of clustering centers, $K_0 \in K$ .
$\mu_i$	The $i$ th clustering center (center of mass), $1 \leq i \leq K$ and $i$ is an integer.
$S_i$	The center of clustering (center of mass) is the $i$ th data set of $\mu_i$ , $1 \leq i \leq K$ and $i$ is an integer.
$x_j$	The $j$ th data, $x_j \in S_i$

- Model Building

$$SSE = \sum_{i=1}^K \sum_{x_j \in S_i} ||x_j - \mu_i||^2 \tag{4}$$

$$minV = \sum_{i=1}^{K_0} \sum_{x_j \in S_i} ||x_j - \mu_i||^2 \tag{5}$$

- K-means clustering algorithm steps
  - (1) Determine  $K_0$  (see Figure 6)

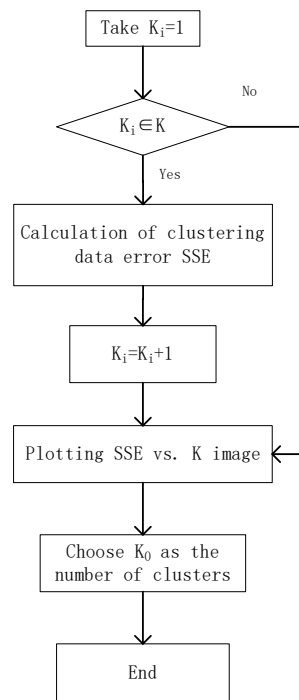


Figure 6. Determining  $K_0$  in the K-means algorithm.

- (2) K-means clustering (see Figure 7)

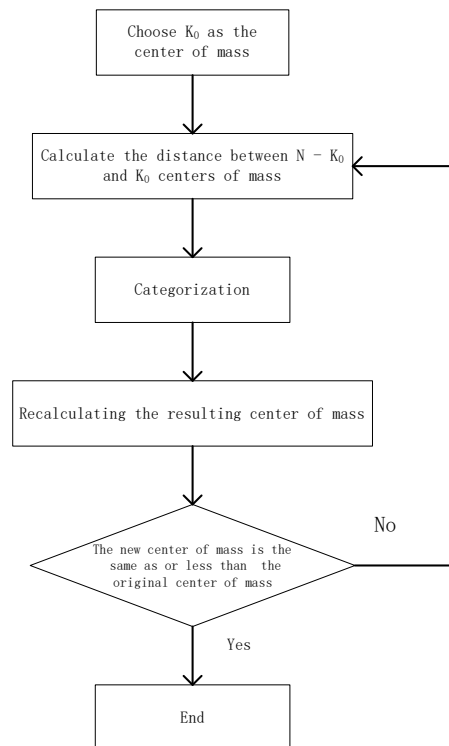


Figure 7. K-means algorithm specific steps.

4.2. NSGA-II Algorithm-Based Node Siting Modeling

1. Basic assumptions

- (1) The calculation cycle is one year.
- (2) Each recycling center can only be handled by one processing center.
- (3) The ratio of inflow to the outflow of express business is 1:1, and the recycling rate is 50%.
- (4) The recycled products are single, all are cartons.
- (5) Straight line approximation instead of actual distance.
- (6) The available vehicles are sufficient, and vehicle path planning and scheduling problems are not considered.
- (7) When the vehicle is from the recycling center to the processing center, only one model can serve, and vice versa, two processes can be served by different models (there are four models 1, 2, 3 and 4, the last two of which are battery-driven), each model has the same rated mass, and the corresponding data are solved according to the full-load state in the calculation.
- (8) The processing center is for rental use.
- (9) Expenses such as equipment purchase, maintenance, and workers' wages are included in the unit processing costs.
- (10) No consideration is given to inventory costs, landfill costs, etc.
- (11) Other parameters such as fixed construction costs for different types of areas are known.
- (12) The express packaging after processing will be transported to each recycling center, and then by each recycling center to each first-level network.
- (13) Only the transportation cost between the recycling center, treatment center, landfill, and paper mill and the carbon emission of the transportation process and treatment process is considered.

• Symbol Description

Symbols	Meaning
$F$	Total cost
$f_1$	Shipping cost
$f_2$	Processing cost
$f_3$	Construction cost
$N$	Number of candidate nodes
$d_{ji}$	The straight-line distance between the $j$ th candidate node and the $i$ th candidate node
$V_{ji}$	Packing volume between the $j$ th candidate node transported to the $i$ th candidate node
$V_i$	Amount of packaging recycling at the $i$ th node
$V_{max}$	The $i$ th node can carry the maximum recycling volume
$m_0$	Mass equivalent per courier package
$t_{rk}$	Freight rate for the $k$ th vehicle unit, $k = 1, 2, 3, 4$
$a_j$	Processing cost using the $j$ th technology unit ( $j = 1,2,3$ )
$C_k$	Regional $k$ unit construction costs, $k = 1, 2, 3, 4$
$c$	Unit storage capacity
$g_1$	CO <sub>2</sub> emissions during transportation
$g_2$	CO <sub>2</sub> emissions from the treatment process
$c_{trk}$	The $k$ th vehicle unit carbon emission factor, $k = 1, 2$
$c_{trk}$	Carbon emission factor per unit for the $k$ th vehicle, $k = 3, 4$
$L_k$	Fuel consumption per unit distance for the $k$ th vehicle, $k = 1, 2$
$L_k$	Electricity consumption per unit distance for the $k$ th vehicle, $k = 3, 4$
$L_k^*$	The fuel consumption per unit distance of the $k$ th vehicle, when fully loaded, $k = 1, 2$
$L_k^*$	The electricity consumption per unit distance of the $k$ th vehicle, when fully loaded, $k = 3, 4$

Symbols	Meaning
$L_k^0$	The fuel consumption per unit distance of the kth vehicle, when unloaded, $k = 1, 2$
$L_k^0$	Electricity consumption per unit distance for the kth vehicle, at no load, $k = 3, 4$
$m$	The kth load capacity
$M$	The kth rated capacity
$c_{arj}$	CO <sub>2</sub> emissions per unit mass of packaging treated with the jth technology, ( $j = 1,2,3$ )
$\alpha$	Reuse rate
$\beta$	Percentage of packaging that is disposed of and transported to landfill
$\gamma$	Percentage of packaging shipped to paper mills after processing

• Objective function

In this paper, the objective function is set from two perspectives: economic and environmental.

- (1) Economic perspective: Since the revenue source of reverse logistics is complicated, government subsidies and profit distribution need to be considered, so only cost minimization is considered in this paper.
- (2) Environmental perspective: to minimize the emissions of CO<sub>2</sub>, one of the greenhouse gases [28–31].

$$\min F = f_1 + f_2 + f_3 \tag{6}$$

$$\min G = g_1 + g_2 \tag{7}$$

$$f_1 = \sum_{i=1}^N \sum_{j=1}^N X_i X_{ji} d_{ji} V_{ji} m_0 t_{rk} + \sum_{i=1}^N X_i d_{im} V_{im} m_0 t_{rk} + \sum_{i=1}^N X_i d_{in} V_{in} m_0 t_{rk} + \sum_{i=1}^N \sum_{j=1}^N X_i X_{ij} d_{ij} V_{ij} m_0 t_{rk} \tag{8}$$

$$f_2 = \begin{cases} a_j V_i m, & V_i m \leq V_{max} m_0 \\ +\infty, & V_{max} m_0 < V_i V_i \end{cases} \tag{9}$$

$$f_3 = \begin{cases} \sum_{i=1}^N X_i V_i m C_1, & i \in \{1, 2, 3\} \\ \sum_{i=1}^N X_i V_i m C_2, & i \in \{4, 5, 6\} \\ \sum_{i=1}^N X_i V_i m C_3, & i \in \{7, 8, 9, 10, 11, 12, 13\} \\ n \sum_{i=1}^N X_i V_i m C_4, & i \in \{14, 15\} \end{cases} \tag{10}$$

$$g_1 = \sum_{i=1}^N \sum_{j=1}^N X_i X_{ji} d_{ji} V_{ji} m_0 L_k c_{trk} + \sum_{i=1}^N X_i d_{im} V_{im} m_0 L_k c_{trk} + \sum_{i=1}^N X_i d_{in} V_{in} m_0 L_k c_{trk} + \sum_{i=1}^N \sum_{j=1}^N X_i X_{ij} d_{ij} V_{ij} m_0 L_k c_{trk} \tag{11}$$

$$L_k = L_k^0 + \frac{L_k^* - L_k^0}{N} m_0 \tag{12}$$

$$g_2 = V_1 m_0 c_{arj} \tag{13}$$

• Constraints

$$X_i = \begin{cases} 1, & \text{The } i\text{th candidate node is selected as the processing center} \\ 0, & \text{The } i\text{th candidate node is selected as the recycling center} \end{cases} \quad (14a)$$

$$X_{ji} = \begin{cases} 1, & \text{The } j\text{th candidate node is assigned to the } i\text{th candidate node} \\ 0, & \text{The } j\text{th candidate node is not assigned to the } i\text{th candidate node} \end{cases} \quad (14b)$$

$$0 \leq V_i \leq V_{max} \quad (15a)$$

$$V_i = V_{ii} + V_{ji} \quad (15b)$$

$$V_i = V_{im} + V_{in} \quad (15c)$$

Equation (6) represents the cost, including transportation cost, construction cost, and treatment cost, in which, transportation cost includes three parts from recycling center to treatment center, treatment center to landfill and paper mill, and treatment center back to the recycling center, construction cost considers four types of areas A, B, C, and D and the cost per unit construction area is different for candidate nodes in different areas, and treatment cost considers alternative of three technologies, and the treatment cost of different technologies is different. Equation (7) represents carbon emissions, including carbon emissions from the transportation process and carbon emissions from the treatment process, where carbon emissions from the transportation process include three parts from recycling center to treatment center, from treatment center to landfill and paper mill, and from treatment center back to the recycling center, and carbon emissions from treatment process consider the three alternative technologies, and the carbon emissions generated by different technologies are different. The above Equation (15a) indicates that the storage volume of node  $i$  takes a range of values, Equation (15b) indicates that node  $i$  is equal to its storage volume plus the volume transported from point  $j$  to point  $i$ , Equation (15c) indicates that the volume transported out of node  $i$  is not greater than the storage volume of node  $i$ . Equations (15a) and (15b) indicate that the above two equations indicate the conservation of flow, the way to achieve each of the above constraints, especially the capacity constraint through the constraint matrix.

According to the relevant information and combined with the actual situation, the following values of the relevant parameters are given in this paper. The values of each variable are as follows in Table 3.

Take fuel consumption per unit distance at no load  $L_1^0 = 0.11$  L/km,  $L_1^* = 0.15$  L/km at full load, carbon emission factor per unit fuel consumption  $c_{tr1} = 2.5$  kg/L, freight per unit  $t_{r1} = 0.001$  CNY/km/kg in vehicle type 1, fuel consumption per unit distance at no load  $L_2^0 = 0.1$  L/km,  $L_2^* = 0.15$  L/km at full load. The carbon emission factor per unit of fuel consumption  $c_{tr2}$  is 2.8 kg/L, the freight cost per unit  $t_{r2}$  is 0.0008, and the electricity consumption per unit distance  $L_3^0$  is 0.1 in vehicle type 2. When vehicle type 3 is empty,  $L_3^* = 0.3$ , when fully loaded, the carbon emission factor per unit of electricity consumption  $c_{tr3}$  is 0.8, the freight cost per unit  $t_{r3}$  is 0.0015, and the electricity consumption per unit distance  $L_4^0 = 0.1$ . When vehicle type 4 is empty,  $L_4^* = 0.3$  when fully loaded, the carbon emission factor per unit of electricity consumption  $c_{tr4} = 0.1$ , unit freight  $t_{r4}$  is 0.0012.

## 5. Algorithm Design

### 5.1. NSGA-II Algorithm Description

#### (1) Chromosome coding

In this paper, we set each generation of the population containing  $n$  individuals, and each individual has only one chromosome, using a repeatable integer coding method, and the total length of the chromosome is 75. From the perspective of corresponding

functions, each chromosome can be divided into five parts, and the length of each part is 15. Specifically, the first part indicates the site selection code, the second part indicates the vehicle type selection code from the recycling center to the treatment center, the third part indicates the vehicle selection code from the processing center to the recycling center, the fourth part indicates the vehicle selection type code from the processing center to the paper mill and the landfill, and the fifth part is the processing technology selection code.

- First part: site selection code

For a generational population, the first part of the chromosome of the  $i$ th ( $1 \leq I \leq n$ , and  $i$  is an integer, the same below) individual, the  $j$ th ( $1 \leq j \leq 15$ , and  $j$  is an integer, the same below) position indicates  $j$  candidate nodes and the value  $k$  corresponding to the  $j$ th position indicates that the  $j$ th candidate node is assigned to node  $k$ , and  $k$  becomes the processing center, where  $k \in \{1 \leq k \leq 15$ , and  $k$  is an integer}.

For example, Figure 8I represents the first part of the chromosome of the first individual of a generation population, whose length is 15, and the value corresponding to the first position is 1, indicating that node 1 is assigned to node 1, i.e., node 1 is selected as a processing center by the candidate node, and so on, and the value corresponding to the 15th position is 15, indicating that node 15 is assigned to node 15, i.e., node 15 is selected as a processing center.

	1	2	3	4	5	6	7	8	9	10	11	12	13	14	15
1	1	2	3	4	5	6	7	8	9	10	11	12	13	14	15

(I)

	1	2	3	4	5	6	7	8	9	10	11	12	13	14	15
7	5	5	5	6	6	6	11	11	11	11	11	13	13	13	13

(II)

15+	1	2	3	4	5	6	7	8	9	10	11	12	13	14	15
1	1	1	1	1	2	2	2	2	3	3	3	4	4	4	4

(III)

15+	1	2	3	4	5	6	7	8	9	10	11	12	13	14	15
7	1	2	3	4	1	2	3	4	1	2	3	4	1	2	3

(IV)

60+	1	2	3	4	5	6	7	8	9	10	11	12	13	14	15
1	1	1	1	1	2	2	2	2	3	3	3	1	1	1	1

(V)

60+	1	2	3	4	5	6	7	8	9	10	11	12	13	14	15
7	1	2	3	1	1	2	3	3	1	2	3	1	1	2	3

(VI)

**Figure 8.** (I,II) indicate the site selection code, (III,IV) indicate the vehicle type selection code from the recycling center to the processing center, the vehicle selection code from the processing center to the recycling center and the vehicle type selection code from the processing center to the paper mill and landfill, (V,VI) are the processing technology selection code.

Figure 8II represents the first part of the chromosome of the 7th individual of this generation population, whose length is 15, and the 1st, 2nd, and 3rd positions correspond to values all of 5, indicating that nodes 1, 2, and 3 are assigned to node 5, i.e., node 5 is

selected as a processing center by the candidate node, and accordingly, nodes 1, 2, and 3 are selected as a recycling center by the candidate node, and so on, and the 12th, 13th, 14th, and 15th positions correspond to the value 13, indicating that nodes 12, 13, 14, and 15 are assigned to node 13, i.e., node 13 is selected as the processing center by the candidate node, and nodes 12, 14, and 15 are selected as the recycling center by the candidate node.

- Second, third, and fourth parts.

For the second part of the  $i$ th ( $1 \leq i \leq n$  and  $i$  is an integer, same below) individual chromosome of a generational population, the value  $l$  corresponding to the  $j$ th ( $16 \leq j \leq 30$  and  $j$  is an integer, same below) position indicates the type of transport vehicle between the  $(j-15)$ th candidate node and the  $k$ th node corresponding to the  $(j-15)$ th position in the first part, where  $l \in \{1 \leq l \leq 4$  and  $l$  is an integer  $\}$  and  $k \in \{1 \leq k \leq 15$  and  $k$  is an integer $\}$ .

For example, Figure 8III represents the second part of the chromosome of the first individual of a generational population which is the same population as the population of Figure 8I with a length of 15. The 16th position corresponds to a value of 1, indicating that the type of the transport vehicle between the first candidate node and the first candidate node corresponding to the first position in the first part is type 1, and so on, and the 30th position corresponds to the value of 4 indicates that the type of the transport vehicle between the 15th candidate node and the 15th candidate node corresponding to the 15th position in the first part is type 4.

Figure 8IV represents the chromosome of the 7th individual of this generation population with a length of 15, and the values corresponding to the 16th, 20th, 24th, and 28th positions are all 1, indicating that the type of transport vehicle between the 1st, 5th, 9th, and 13th candidate nodes and the 5th, 6th, 11th, and 13th candidate nodes corresponding to the first part is all type 1, and the values corresponding to the 17th, 21st, 25th, and 29th positions are 2, indicating that the vehicle types of the transport vehicles between the 2nd, 6th, 10th, and 14th candidate nodes and the corresponding 2nd, 6th, 10th, and 14th candidate nodes in the first part are all of type 2, and the remaining cases and so on.

- Fifth part.

For the  $i$ th ( $1 \leq i \leq n$ ,  $i$  is an integer, the same below) individual chromosome of the fifth part of a generational population, the value  $p$  corresponding to the  $j$ th ( $61 \leq j \leq 75$ ,  $j$  is an integer, the same below) position denotes the  $p$ th technique chosen for the  $k$ th node corresponding to the  $(j-15)$ th position of the first part, where  $p \in \{1 \leq p \leq 3$  and  $p$  is an integer $\}$  and  $k \in \{1 \leq k \leq 15$  and  $k$  is an integer $\}$ . For example, Figure 8V represents the fifth part of the chromosome of the first individual of a generational population (this population is the same population as the population in Figure 8), whose length is 15, and the 61st position corresponds to a value of 1, indicating the  $j$ 60th candidate node, i.e., the first candidate node uses technology 1, and so on, and the 75th position corresponds to a value of 1, indicating the  $j$ 60th candidate node i.e., the 15th candidate node also adopts technique 1.

Figure 8VI represents the chromosome of the seventh individual of this generation population with a length of 15, and the values corresponding to the 61st, 64th, 65th, 69th, 72nd, and 73rd positions are all 1, indicating that the 1st, 4th, 5th, 9th, 12th, and 13th candidate nodes corresponding to the first part adopt technology 1, and the values corresponding to the 62nd, 66th, 70th, and 74th positions are all 2, indicating that the 2nd, 6th, 10th, and 14 candidate nodes adopt technique 2, and the values corresponding to the 63rd, 67th, 68th, 71st, and 75th positions are all 3, indicating that the 3rd, 7th, 8th, 11th, and 15th candidate nodes adopt technique 3.

## (2) Population initialization

According to the above coding method, in this paper, let there be  $n = 50$  individuals per generation of population, each individual has only one chromosome, and the length of each chromosome is 75, i.e.,  $m = 75$ , the first part corresponds to the candidate processing center coding, each position randomly generates a repeatable integer  $k$  ( $1 \leq k \leq 15$ ), the second, third, and fourth parts correspond to the vehicle type coding, each position ran-

domly generates a repeatable integer  $l$  ( $1 \leq l \leq 4$ ), the fifth part corresponds to the type of technology used,  $p \in \{1 \leq l \leq 3, \text{ and } p \text{ is an integer}\}$ .

(3) Adaptation degree function

In this paper, the fitness of each individual is calculated according to the rank size and crowding degree of the non-dominated stratum, specifically, the parents and children are merged, the new population after the merger is non-dominated stratified, and the crowding degree is calculated for all individuals, and finally, the individuals are selected according to the principle that priority is given to individuals with small non-dominated stratification rank and priority is given to individuals with large crowding degree in the same stratum until the population number is satisfied requirements, the method has a slightly different logic from the classical NSGA-II algorithm, but is identical in purpose and fully equivalent in effect [32–34].

(4) Crossover operation [35]

In this paper, the simulated binary crossover method is used to perform crossover operations on population chromosomes. Assuming that the children generated by the crossover of parents  $x_a$  and  $x_b$  are  $y_a$  and  $y_b$ , then for the  $k$ th position of children  $y_a$  and  $y_b$  we have.

$$y_a(k) = \frac{1}{2}[(1 + \beta)x_a(k) + (1 - \beta)x_b(k)] \tag{16}$$

$$y_b(k) = \frac{1}{2}[(1 - \beta)x_a(k) + (1 + \beta)x_b(k)] \tag{17}$$

Among them,

$$\beta = \begin{cases} 2r^{\frac{1}{1+\eta}}, r \leq 0.5 \\ (2 - 2r)r^{-\frac{1}{1+\eta}}, r > 0.5 \end{cases} \tag{18}$$

In the above equation,  $r \sim U [0, 1]$ ,  $\eta$  is a custom parameter, and the larger the value, the closer the offspring is to the parent.

In this paper, we take  $\eta = 20$ , and for crossover, the first half of individuals and the second half of individuals in each generation of the population are combined two by two, and when the number of individuals is odd, the last individual does not participate in the crossover.

(5) Variation operation

In this paper, the polynomial variation method is used to perform various operations on population chromosomes; specifically, the variation form is,

$$v'_k = v_k + \delta(u_k - l_k) \tag{19}$$

Among them,

$$\delta = \begin{cases} \left[ 2u + (1 - 2u)(1 - \delta_1)^{\eta_m + 1} \right]^{\frac{1}{\eta_m + 1}} - 1, u \leq 0.5 \\ 1 - \left[ 2(1 - u) + 2(u - 0.5)(1 - \delta_2)^{\eta_m + 1} \right]^{\frac{1}{\eta_m + 1}}, u > 0.5 \end{cases} \tag{20}$$

In the above equation,  $\delta_1 = (v_k - l_k)/(u_k - l_k)$ ,  $\delta_2 = (v_k - v_k)/(u_k - l_k)$ ,  $u$  is a random number in the interval  $[0, 1]$ ,  $\eta_m$  is a custom parameter, and this paper takes  $\eta_m = 20$ .

5.2. NSGA-II Algorithm Steps

Step 1: encoding by repeatable integer coding.

Step 2: initialize the population and generate a population containing  $m$  individuals, each containing one chromosome, at this point, set as the initial population.

Step 3: non-dominated stratification of the individuals of the initial population.

Step 4: calculate the fitness of the individuals of the initial population based on the results of the non-dominated stratification in step 3.



Step 5: select a certain number of individuals in the initial population as the evolutionary generation 0 according to the calculation result in step 4, and all individuals of the initial population are selected as generation 0 in this paper.

Step 6: start evolution, take generation  $i$  ( $i \in \{0 \leq i < 50$  and  $k$  is an integer}) as the parent, perform crossover and mutation operations on the individuals of the parent to generate the children corresponding to the parent of generation  $i$ , and fuse the individuals of the parent and children of generation  $i$ .

Step 7: decode the fused individuals from step 6 and calculate the objective function values of the fused individuals.

Step 8: non-dominated stratification of the fused individuals from step 6 and calculation of their crowding degree.

Step 9: according to the calculation result of step 8, select  $m$  individuals as the  $(i + 1)$ th generation according to the non-dominated stratification level from the lowest to the highest and when the same level according to the crowding degree from the largest to the smallest, and return to step 6 if the required number of evolutionary iterations is not satisfied.

Step 10: the  $(i + 1)$ th generation of individuals has been noted as the Pareto solution and the corresponding solution is the Pareto frontier solution [36–38].

The algorithm terminates.

The basic flow chart of the algorithm is shown in the following Figure 9.

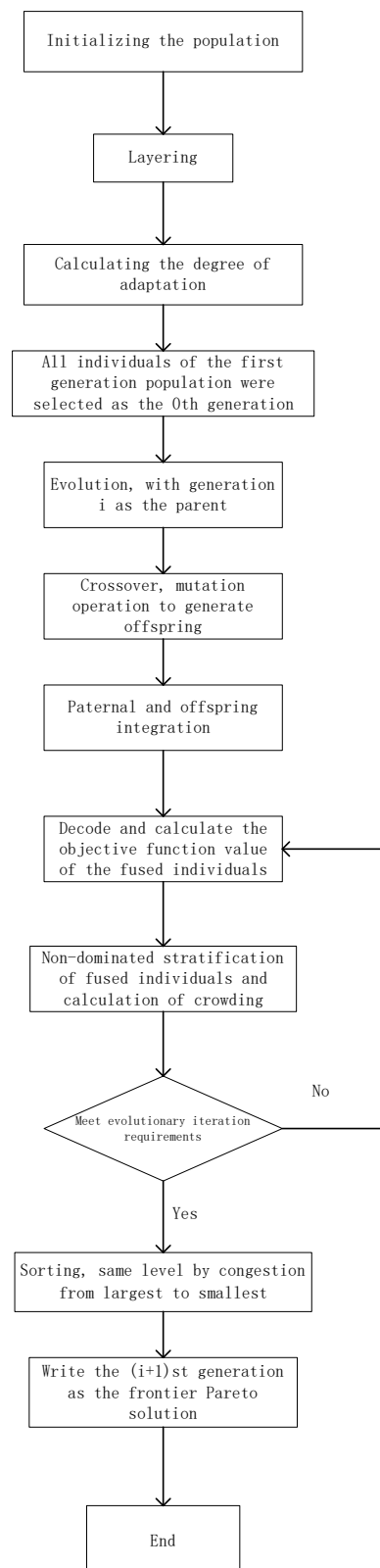


**Figure 9.** The basic process of mutation operation.

## 6. Analysis of Results

### 6.1. Candidate Points

(1) Execution of the algorithm yields the SSE versus K plot, as shown in Figure 10.

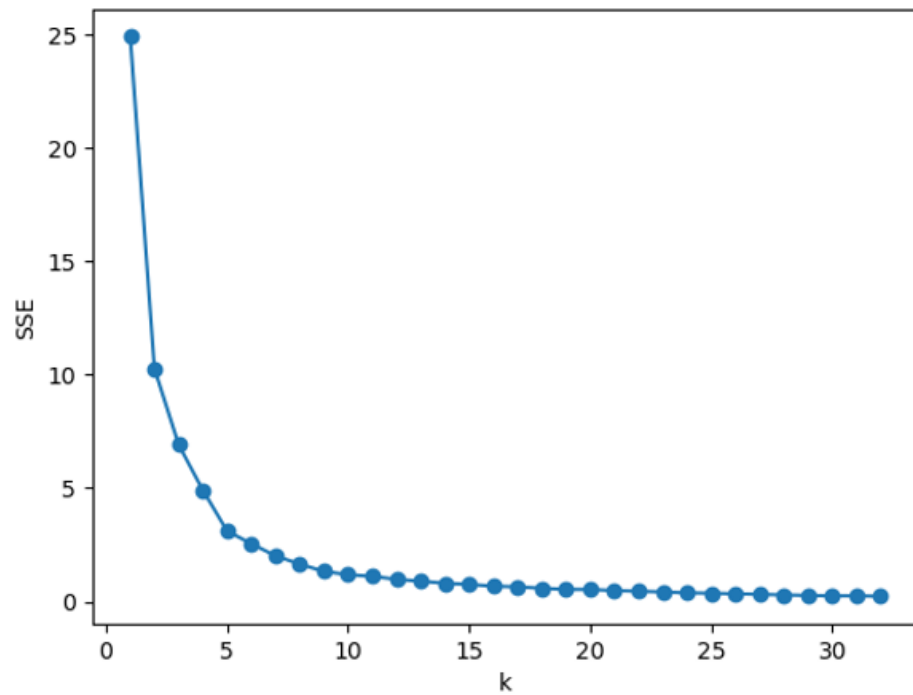


Figure 10. SSE versus K.

From the above Figure 8, it can be seen that the inflection point appears between  $K = 5$  and  $K = 10$ . It is known from the rule of elbow law that  $K_0 = 15$  should satisfy  $5 \leq K_0 \leq 10$ , but considering the actual demand,  $K_0$  can be expanded appropriately by the rule of on-demand selection law, and  $K_0 = 15$  is taken in this paper.

(2) Take  $K_0 = 15$ , execute K-means algorithm, get 15 clustering centers, and use them as candidate processing centers, whose latitude and longitude information is shown in Table 4, and the location schematic is shown in Figure 11.

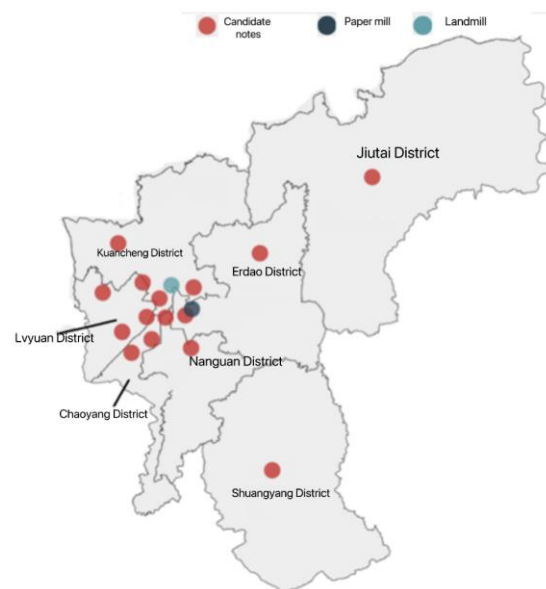


Figure 11. Schematic diagram of the location of the candidate nodes, paper mill, and landfill.

**Table 4.** Latitude and longitude of candidate nodes.

Serial Number	Latitude/°N	Longitude/°E	Serial Number	Latitude/°N	Longitude/°E
1	44.20957	125.9666	9	43.89134	125.3411
2	43.85894	125.2093	10	43.97082	125.2716
3	43.54504	125.6638	11	43.9477	125.1507
4	43.84200	125.2989	12	43.95960	125.4261
5	44.05939	125.1975	13	44.03693	125.6269
6	43.82241	125.4182	14	43.89649	125.4009
7	43.89262	125.2839	15	43.81163	125.2380
8	43.93453	125.3227			

6.1.1. Classification of Candidate Nodes in Region M

Considering the economic development status of seven districts, this paper delineates four categories of regions A, B, C, and D, as shown in Figure 12.



**Figure 12.** Schematic diagram of candidate node sub-region location.

According to the above classification results, the regions to which each candidate node belongs are shown in Table 5.

**Table 5.** Classification regions and administrative regions to which each candidate node belongs.

Candidate Nodes	Classification Area	Administrative District	Candidate Nodes	Classification Area	Administrative District
1	A	Kuancheng District	9	C	Lvyuan District
2	A	Nanguan District	10	C	Kuancheng District
3	A	Lvyuan District	11	C	Kuancheng District
4	B	Lvyuan District	12	C	Nanguan District
5	B	Erdao District	13	C	Erdao District
6	B	Chaoyang District	14	D	Jiutai District
7	C	Chaoyang District	15	D	Shuangyang District
8	C	Lvyuan District			

6.1.2. Determination of The Distance between Candidate Nodes

The latitude and longitude of 15 nodes can be known from Table 3, and the distance between any two points  $(L_1, N_1)$  and  $(L_2, N_2)$  is calculated using Equation (20) to obtain the distance between each candidate node, as shown in Table 6.

$$d = \sqrt{[111(N_1 - N_2)]^2 + \{111[E_1 \cos(N_1) - E_2 \cos(N_2)]\}^2} \tag{21}$$

Table 6. Distance between candidate nodes.

Serial Number	1	2	3	4	5	6	7	8
23.86859	0	40.23685	12.67707	23.22249	44.70217	29.2916	73.10302	13.03013
16.60001	40.23685	0	29.87562	18.59793	6.318052	10.96083	113.3377	27.81905
13.40235	12.67707	29.87562	0	11.51298	33.4658	19.47316	84.28883	3.378439
3.75025	23.22249	18.59793	11.51298	0	21.95307	9.150016	95.73491	10.19329
20.84032	44.70217	6.318052	33.4658	21.95307	0	16.03422	117.6109	31.87447
6.106751	29.2916	10.96083	19.47316	9.150016	16.03422	0	102.3944	17.09786
96.87778	73.10302	113.3377	84.28883	95.73491	117.6109	102.3944	0	85.74007
11.22128	13.03013	27.81905	3.378439	10.19329	31.87447	17.09786	85.74007	0
39.59672	63.28908	23.0548	52.68995	41.21885	19.52163	34.00031	136.3915	50.81169
4.792569	19.34723	20.89395	10.23743	6.236652	25.49322	9.973975	92.44419	7.36417
8.717617	16.11011	24.30006	9.500052	9.929159	29.18902	13.34816	89.14593	6.131975
35.19108	48.15778	30.43948	45.10163	38.93564	35.71272	30.90118	114.8546	41.757
16.30645	30.78207	18.70151	25.93917	20.0393	25.01903	13.35269	101.709	22.63918
7.435185	27.15075	14.28599	19.15585	11.17926	20.04865	4.903537	99.99842	16.22207
0	23.86859	16.60001	13.40235	3.75025	20.84032	6.106751	96.87778	11.22128
Serial Number	9	10	11	12	13	14	15	
1	63.28908	19.34723	16.11011	48.15778	30.78207	27.15075	23.86859	
2	23.0548	20.89395	24.30006	30.43948	18.70151	14.28599	16.60001	
3	52.68995	10.23743	9.500052	45.10163	25.93917	19.15585	13.40235	
4	41.21885	6.236652	9.929159	38.93564	20.0393	11.17926	3.75025	
5	19.52163	25.49322	29.18902	35.71272	25.01903	20.04865	20.84032	
6	34.00031	9.973975	13.34816	30.90118	13.35269	4.903537	6.106751	
7	136.3915	92.44419	89.14593	114.8546	101.709	99.99842	96.87778	
8	50.81169	7.36417	6.131975	41.757	22.63918	16.22207	11.22128	
9	0	43.94864	47.30247	39.51704	38.13702	36.7922	39.59672	
10	43.94864	0	3.958057	35.54501	16.25327	8.920409	4.792569	
11	47.30247	3.958057	0	35.63389	16.58221	11.11113	8.717617	
12	39.51704	35.54501	35.63389	0	19.29206	27.75662	35.19108	
13	38.13702	16.25327	16.58221	19.29206	0	9.082896	16.30645	
14	36.7922	8.920409	11.11113	27.75662	9.082896	0	7.435185	
15	39.59672	4.792569	8.717617	35.19108	16.30645	7.435185	0	

6.1.3. Determination of the Candidate Node Express Volume

According to the previous data, the design values were weighted according to the average ratio of the population in the seven districts of the M region to the total population of Changchun, and the results are shown in Table 7.

The classification results of the candidate nodes, Nanguan District has one class A and C regional nodes, respectively, candidate nodes 2 and 12, known from Table 1 Nanguan District express the business volume of 103,352,300 pieces. This paper assumes that the ratio of A and C regional nodes express business volume in Nanguan District is 7: 3, then the express business volume of candidate nodes 2 and 12 are 7234.65967 and 3100.56843 million pieces. According to the above rules, the express business volume of each candidate node is shown in Table 8.

**Table 7.** Express business volume by district.

Administrative District	Express Business Volume/Million Pieces
Nanguan District	103.3523
Kuancheng District	90.56302
Chaoyang District	103.4675
Erdao District	79.95588
Lvyuan District	90.23914
Shuangyang District	50.62379
Jiutai District	92.637

**Table 8.** Express the business volume of each candidate node.

Candidate Nodes	Express Business Volume/ Million Pieces	Candidate Nodes	Express Business Volume/ Million Pieces
1	54.33781	9	9.023914
2	72.3466	10	18.1126
3	45.11957	11	18.1126
4	27.07174	12	31.00568
5	47.97353	13	31.98235
6	62.08048	14	50.62379
7	41.38699	15	92.637
8	9.023914		

6.2. Number of Iterations, Crossover Variance Probability Selection

In this paper, we use Python 3.8.5 for algorithm implementation, in which some sub-functions directly call the functions of the Geatpy library, such as selection sub-functions and crossover sub-functions.

In this paper, we set the number of population individuals  $m = 100$  and  $M = 3000$ , in the actual problem, the number of iterations will have a large impact on the performance of the whole algorithm, so in this paper, the two single objectives of total cost and carbon dioxide total emission, as shown in Figure 13, where the blue line indicates the average value and the red line indicates the minimum value, it can be seen that both the average value and the minimum value decrease gradually with the increase of the number of generations and tend to be stable, and both objective functions show good convergence, so it is feasible to take  $M = 3000$ .

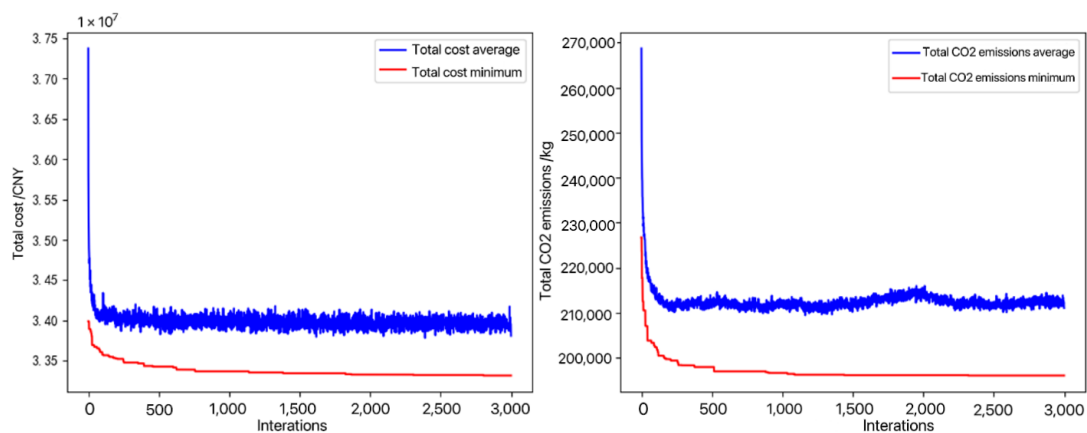


**Figure 13.** Plot of the total cost–number of iterations, total carbon dioxide emissions–number of iterations  $c$  ( $M = 3000$ ).

In this paper, we compare and analyze the relevant indicators for four cases with cross-variance probabilities of 0.9, 0.8, 0.7, and 0.6. Total cost vs. total carbon dioxide

emissions relationship diagram (cross-variance probability is 0.9, 0.8, 0.7, 0.6) as shown in Figure 14A–D and Table 9.

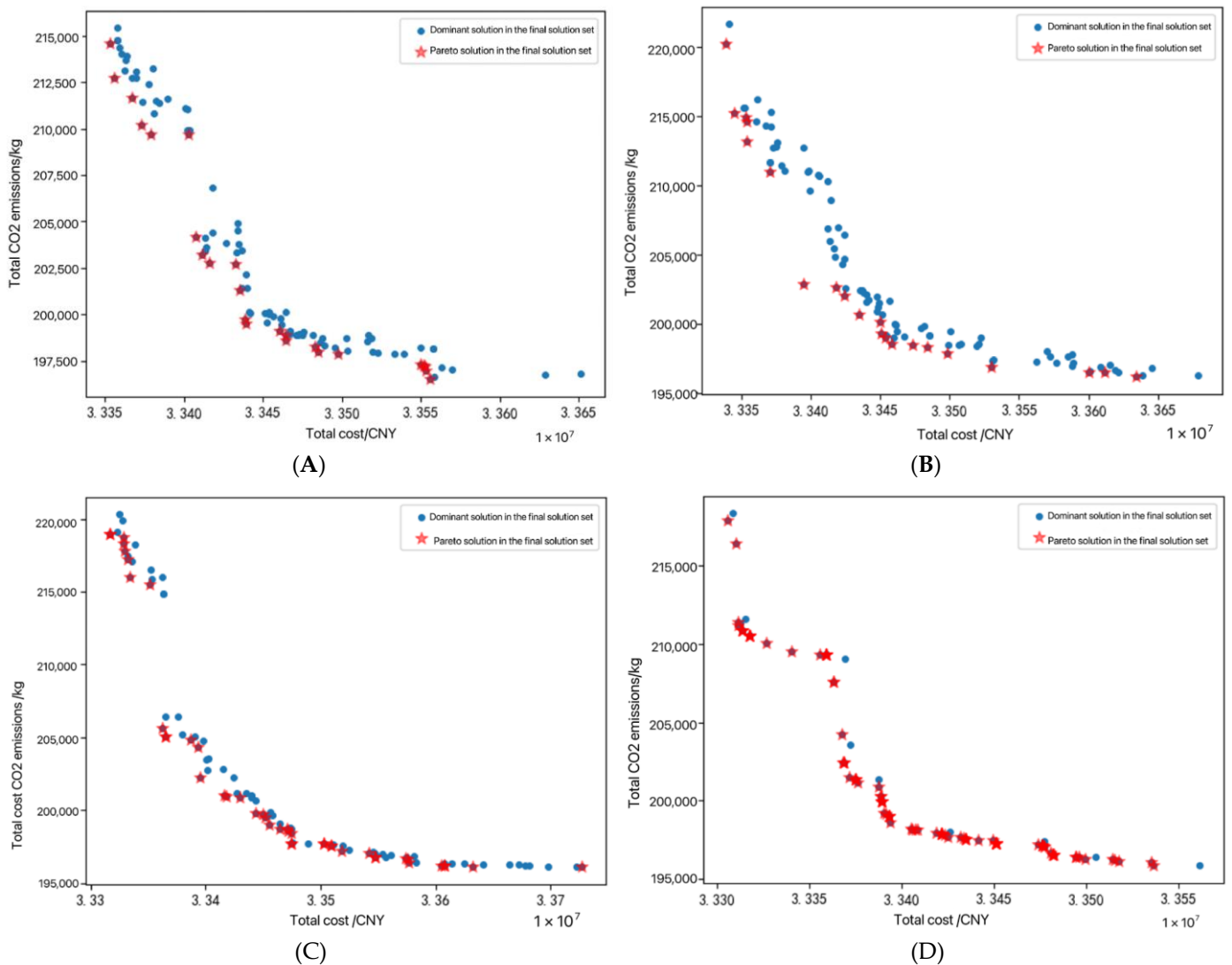


**Figure 14.** (A) Total cost vs. total carbon dioxide emissions relationship diagram (cross-variance probability is 0.9). (B) Total cost and total carbon dioxide emissions relationship diagram (cross-variance probability is 0.8). (C) Total cost versus total carbon dioxide emissions relationship diagram (cross-variance probability is 0.7). (D) Total cost and total carbon dioxide emissions relationship diagram (cross-variance probability is 0.6).

**Table 9.** Correlation indicators.

Cross-Variance Probabilities	Indicator Name	Percentage of Non-Dominated Solutions	HV	Spacing
0.9	Numerical value	0.24	0.016768	3312.822067
0.8	Numerical value	0.21	0.019379	3649.327564
0.7	Numerical value	0.43	0.019267	2713.471153
0.6	Numerical value	0.88	0.017934	3232.380758

Note: After testing, each index fluctuates somewhat during repeated calculations, and the best value in each calculation process is taken.

Integrating the three indicators of non-dominated solution percentage, HV, and Spacings, and the final three generated images, this paper selects the case of  $M = 3000$  and the probability of cross-variance is 0.7 for analysis, and pools the analysis results to give management suggestions. According to the results of the selection of the number of iterations, this paper runs the procedure at  $M = 3000$  and the cross-variance probability is 0.7, and a total of 43 Pareto solutions are obtained, as shown in Figure 15, which can be more clearly seen in the Pareto frontier solutions [39,40].

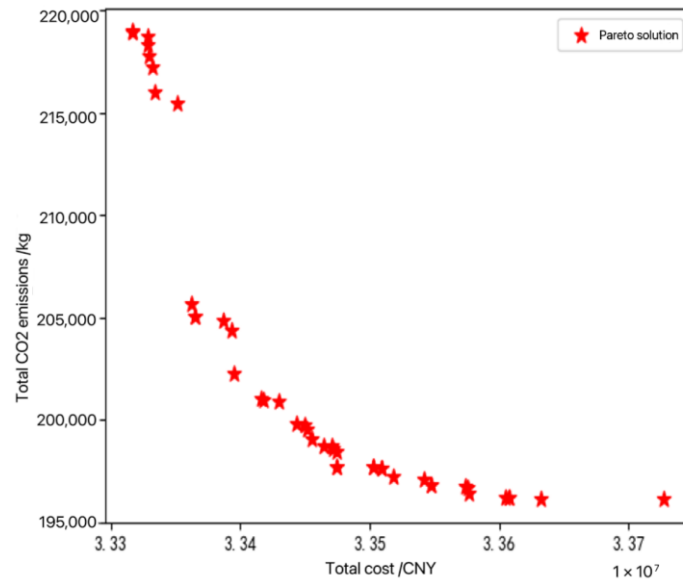


Figure 15. Total cost and carbon dioxide emissions Pareto solution set.

For further analysis, the obtained Pareto solution sets can be classified into I, II, and III, as shown in Figure 16.

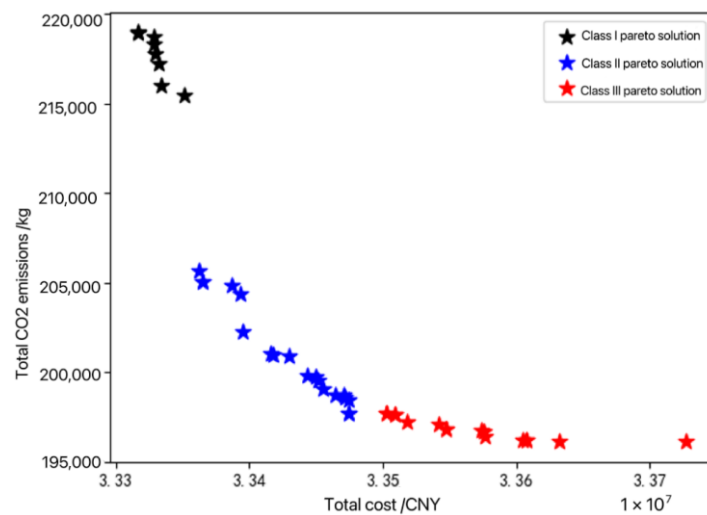


Figure 16. Classification of total cost and total carbon dioxide emissions ( $M = 3000$ ) Pareto solution set.

Among them, the total cost of class I is at a low level and carbon emission is at a high level, the total cost and carbon emission of class II are both at a medium level, and the total cost of class III is at a high level and carbon emission is at a low level. For different development stages of recycling system construction and development, different solution sets of different regions can be selected as design solutions under the consideration of total



cost and carbon emission only. When the whole society’s recycling system has developed to a certain extent, Region III can be chosen.

In this paper, one point from each of the three categories I, II, and III is randomly selected for analysis, and the selected points are shown in Figure 17.

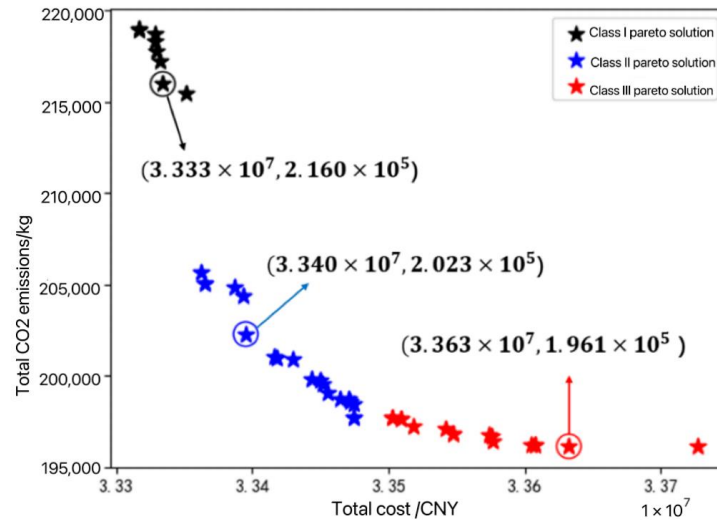


**Figure 17.** Schematic diagram of sample solution selection for the Pareto solution of total cost and total carbon dioxide emissions ( $M = 3000$ ).

The coordinates of the point selected for Class I are  $(3.333 \times 10^7, 2.160 \times 10^5)$ , which is noted as the sample solution for Class I, i.e., the total cost is  $3.333 \times 10^7$  CNY and carbon emission is  $2.160 \times 10^5$  kg. The first, second, third, and fourth parts of the chromosome corresponding to this point are coded as

$$\begin{aligned}
 & [14 \ 10 \ 4 \ 7 \ 11 \ 7 \ 4 \ 14 \ 5 \ 14 \ 14 \ 13 \ 13 \ 12 \ 14 \ ] \\
 & \quad [2 \ 1 \ 1 \ 2 \ 3 \ 4 \ 2 \ 4 \ 4 \ 1 \ 3 \ 4 \ 4 \ 2 \ 4 \ ] \\
 & \quad [2 \ 2 \ 3 \ 1 \ 2 \ 1 \ 2 \ 2 \ 4 \ 2 \ 2 \ 1 \ 2 \ 1 \ 2 \ ] \\
 & \quad [3 \ 3 \ 1 \ 2 \ 3 \ 1 \ 3 \ 4 \ 3 \ 2 \ 4 \ 2 \ 3 \ 4 \ 4 \ ] \\
 & \quad [2 \ 3 \ 2 \ 1 \ 3 \ 2 \ 3 \ 3 \ 1 \ 1 \ 3 \ 3 \ 3 \ 3 \ 3 \ ]
 \end{aligned}$$

According to the algorithm design rules, the above code is decoded to obtain the recycling center responsible for each processing center, the model used, and the technology used, as shown in Table 10 (for convenience, Table 11 notes the recycling center to the processing center as Section 1, the processing center back to the recycling center as Section 2, and the processing center to the landfill and paper mill as Section 3, the same as the following table). The location of each node is shown in Figure 18A.

**Table 10.** Class I sample solution analysis.

Processing Center	Recycling Center in Charge	Road Section			Technical Processing
		1	2	3	
4	3	1	3	1	1
5	9	4	4	3	1
7	4, 6	2, 4	1, 1	2, 1	1, 2
10	2	1	2	3	3
11	5	3	2	3	3
12	14	2	1	4	3
13	12, 13	4, 4	1, 2	2, 3	3, 3
14	1, 8, 10, 11, 15	2, 4, 1, 3, 4	2, 2, 2, 2, 2	3, 4, 2, 4, 4	2, 3, 1, 3, 3

Table 11. Class II sample solution analysis.

Processing Center	Recycling Center in Charge	Road Section			Technical Processing
		1	2	3	
3	7	2	2	3	3
4	3	2	2	3	3
5	9	4	4	2	2
6	1	4	2	3	3
7	4, 6	2, 2	1, 1	2, 1	2, 3
10	2	2	2	3	3
11	5	3	2	4	3
12	14	1	1	3	3
13	13	4	2	3	3
14	8, 10, 11, 12, 15	4, 1, 3, 4, 4	2, 1, 2, 2, 2	4, 4, 3, 3, 4	3, 2, 3, 3, 3

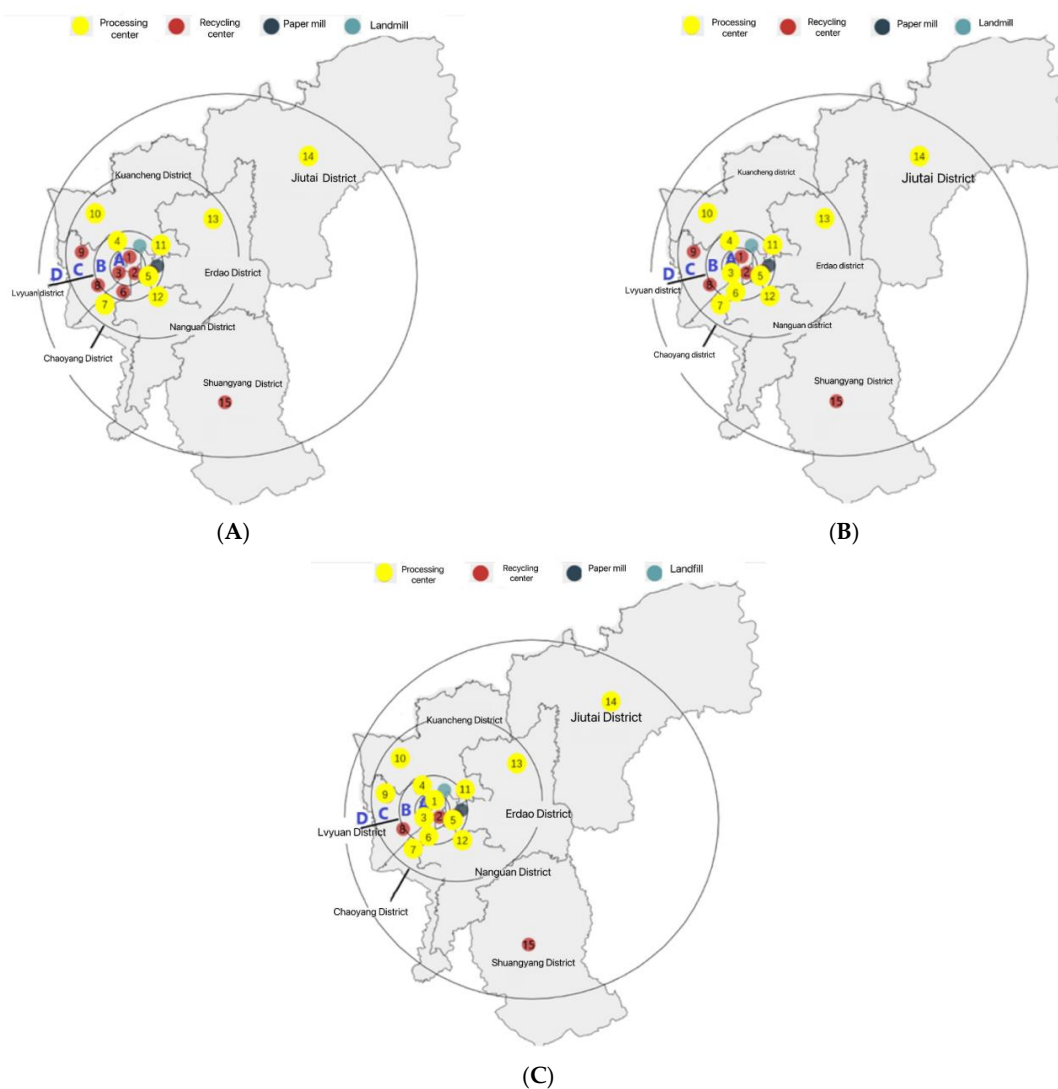


Figure 18. (A) Schematic diagram of the location of each node of the class I sample solution. (B) Schematic diagram of the location of each node of the class II sample solution. (C) Location diagram of nodes of Class III sample solutions.

The coordinates of the point selected for class II are  $(3.340 \times 10^7, 2.023 \times 10^5)$ , which is noted as the sample solution for class II, i.e., the total cost is  $3.340 \times 10^7$  CNY and the carbon emission is  $2.023 \times 10^5$  kg. The first, second, third, and fourth parts of the chromosome corresponding to this point are coded as

$$\begin{aligned}
 & [ 6 \ 10 \ 4 \ 7 \ 11 \ 7 \ 3 \ 14 \ 5 \ 14 \ 14 \ 13 \ 13 \ 12 \ 14 ] \\
 & \quad [ 4 \ 2 \ 1 \ 2 \ 3 \ 2 \ 2 \ 4 \ 4 \ 1 \ 3 \ 4 \ 4 \ 1 \ 4 ] \\
 & \quad [ 2 \ 2 \ 3 \ 1 \ 2 \ 1 \ 2 \ 2 \ 4 \ 1 \ 2 \ 2 \ 2 \ 1 \ 2 ] \\
 & \quad [ 3 \ 3 \ 1 \ 2 \ 4 \ 1 \ 3 \ 4 \ 2 \ 4 \ 3 \ 3 \ 3 \ 3 \ 4 ] \\
 & \quad [ 3 \ 3 \ 2 \ 2 \ 3 \ 3 \ 3 \ 3 \ 2 \ 2 \ 3 \ 3 \ 3 \ 3 \ 3 ]
 \end{aligned}$$

The above codes were decoded to obtain the recycling centers responsible for each processing center, the models used, and the technologies used, as shown in Table 11. The location of each node is shown in Figure 18B.

The coordinates of the point selected for class III are  $(3.363 \times 10^7, 1.961 \times 10^5)$ , which is noted as the sample solution for class III, i.e., total cost is  $3.363 \times 10^7$  CNY and carbon emission is  $1.961 \times 10^5$  kg. The first, second, third, and fourth parts of the chromosome corresponding to this point are coded as,

$$\begin{aligned}
 & [ 6 \ 10 \ 4 \ 7 \ 11 \ 12 \ 3 \ 14 \ 5 \ 9 \ 14 \ 1 \ 13 \ 12 \ 7 ] \\
 & \quad [ 3 \ 4 \ 3 \ 3 \ 3 \ 4 \ 2 \ 4 \ 2 \ 2 \ 3 \ 3 \ 4 \ 4 \ 4 ] \\
 & \quad [ 1 \ 2 \ 3 \ 1 \ 3 \ 3 \ 2 \ 2 \ 4 \ 1 \ 4 \ 2 \ 2 \ 1 \ 2 ] \\
 & \quad [ 3 \ 3 \ 1 \ 2 \ 3 \ 2 \ 3 \ 3 \ 3 \ 4 \ 4 \ 4 \ 3 \ 3 \ 3 ] \\
 & \quad [ 2 \ 3 \ 2 \ 2 \ 3 \ 2 \ 3 \ 3 \ 2 \ 1 \ 3 \ 3 \ 3 \ 3 \ 2 ]
 \end{aligned}$$

After the above encoding and decoding, the recycling centers, models, and technologies adopted by each processing center are obtained, as shown in Table 12. The location of each node is shown in Figure 18(C).

Table 12. Class III sample solution analysis.

Processing Center	Recycling Center in Charge	Road Section			Technical Processing
		1	2	3	
1	12	3	2	4	3
3	7	2	2	3	3
4	3	3	3	1	2
5	9	2	4	3	2
6	1	3	1	3	2
7	4, 15	3, 4	1, 2	2, 3	2, 2
9	10	2	1	4	1
10	2	4	2	3	3
11	5	3	3	3	3
12	6, 14	4, 4	4, 1	2, 3	2, 3
13	13	4	2	3	3
14	8, 11	4, 3	2, 4	3, 4	3, 3

Compare and analyze the sample solutions of class I, II, and III selected above: From the perspective of site selection, it can be seen that among the nodes selected by class I sample solutions, 2 nodes are located in region B, 5 nodes are located in region C, and 1 node is located in region D. Among the nodes selected by region B sample solutions, 1 node is located in region A, 3 nodes are located in region B, 5 nodes are located in region C, and 1 node is located in region D. Among the nodes selected by class III sample solutions,

2 nodes are located in region A, 4 are located in region B, 5 are located in region C, and 1 is located in region D, and the node selected by the sample solution of class III contains class II, and class II contains class I. From the perspective of the selected vehicle types, excluding some invalid codes such as starting and ending points being the same node, it can be seen that the transportation modes between nodes are widely selected, and all four types of vehicles have been applied. From the perspective of the selected technology, it can be seen that the same processing center can choose 2 or more kinds of processing technology, and each processing technology has an application. To sum up, after selecting the regional category, the specific location, vehicle type, and technology should be taken into consideration to optimize the whole system.

## 7. Conclusions

Green and low-carbon products are becoming increasingly popular, and green carbon reduction has become the mainstream way of consumption upgrading. This paper analyzes and summarizes the existing courier packaging recycling model, and establishes a new courier packaging recycling model based on the concept of sharing from a low-carbon perspective. From the perspective of engineering research, this paper proposes a complete set of reverse logistics network design process for express packaging, especially from the existing express network, and establishes a network optimization model by combining qualitative and quantitative analysis, which provides a certain technical reference value for similar projects. From the application value point of view, this paper defines the scope of region M. According to the population of each administrative region in region M, the design value is used to weight according to the population number to estimate the courier volume of each administrative region in region M. The location information of 535 courier points in region M was obtained and filtered. The courier packaging recycling mode adopted in region M was determined. This paper also randomly selects one sample solution from each of the three types of solution sets, conducts the coding interpretation of site selection, vehicle selection, and processing technology selection and gives an example design scheme. The express packaging recycling network constructed in this paper can avoid the waste of express packaging, reduce environmental pollution, and promote the sustainable development of social environment and economy for the social development of region M. For the express enterprises in region M, it can improve the utilization rate of express packaging, reduce the cost, actively assume social responsibility, and establish a good corporate image. There are shortcomings in this paper. Affected by the epidemic, there are large errors in the estimation of express business volume in each administrative region of M. The performance of the program written by the relevant algorithm is unstable, and the time complexity and space complexity are not considered, and the algorithm design and program writing should be further optimized. In future research, this aspect should be considered more comprehensively and carefully.

**Author Contributions:** Conceptualization, J.M. and J.C.; methodology, J.C.; software, J.C.; validation, X.L. and H.Z.; formal analysis, J.C. and C.L.; investigation, J.M.; resources, X.L.; data curation, J.C.; writing—original draft preparation, J.C.; writing—review and editing, H.Z.; visualization, C.L. and X.L.; supervision, C.L. and H.Z.; project administration, H.Z. and C.L. All authors have read and agreed to the published version of the manuscript.

**Funding:** This research received no external funding.

**Data Availability Statement:** Not applicable.

**Acknowledgments:** The authors thank the editor and the anonymous referees for their helpful comments and critics, and Professor Guangdong Tian for helpful discussions and guidance.

**Conflicts of Interest:** The authors declare no conflict of interest.

### Appendix A

**Table A1.** Total population of each district in Region M.

Name of Administrative Region	Year		
	2020	2019	2018
Nanguan District	764,163	744,357	717,550
Kuancheng District	663,020	651,892	645,688
Chaoyang District	758,991	747,508	729,875
Erdao District	580,277	579,356	577,012
Lvyuan District	651,635	654,046	659,108
Shuangyang District	364,782	366,780	371,912
Jiutai District	667,942	671,291	679,336
Total population of Changchun	7,537,969	7,512,896	7,511,748

**Table A2.** The proportion of the population of each district in the total population of Changchun in M region.

Name of Administrative Region	The Percentage of the Population in the Current Year			
	2020	2019	2018	2018–2020
Nanguan District	10.14%	9.91%	9.55%	9.95%
Kuancheng District	8.80%	8.68%	8.60%	8.72%
Chaoyang District	10.07%	9.95%	9.72%	9.96%
Erdao District	7.70%	7.71%	7.68%	7.70%
Lvyuan District	8.64%	8.71%	8.77%	8.69%
Shuangyang District	4.84%	4.88%	4.95%	4.87%
Jiutai District	8.86%	8.94%	9.04%	8.92%

**Table A3.** Location of express points in Nanguan District.

Serial Number	Latitude/°N	Longitude /°E	Serial Number	Latitude/°N	Longitude/°E
1	43.837454	125.327664	51	43.85571	125.400205
2	43.789996	125.437189	52	43.843923	125.425986
3	43.88474	125.350858	53	43.803751	125.315023
4	43.893736	125.35813	54	43.750018	125.409793
5	43.834801	125.333301	55	43.899874	125.332733
6	43.827144	125.329905	56	43.827882	125.414442
7	43.840422	125.373367	57	43.878994	125.336723
8	43.826949	125.375575	58	43.896309	125.351509
9	43.882053	125.349496	59	43.882392	125.347125
10	43.842641	125.374858	60	43.905428	125.342984
11	43.906604	125.343757	61	43.861626	125.359128
12	43.844766	125.380254	62	43.844444	125.38038
13	43.813458	125.457464	63	43.813495	125.465922
14	43.897753	125.338467	64	43.802057	125.283431
15	43.782392	125.406786	65	43.85151	125.450023
16	43.820709	125.314338	66	43.891005	125.339234
17	43.842253	125.40775	67	43.903562	125.344714
18	43.827599	125.32845	68	43.891354	125.337182
19	43.830943	125.309065	69	43.81103	125.400753
20	43.879202	125.334329	70	43.835494	125.433065
21	43.827144	125.329905	71	43.789372	125.375345
22	43.796082	125.309145	72	43.871081	125.353375
23	43.869381	125.339793	73	43.893203	125.350009
24	43.839403	125.356681	74	43.897777	125.345988
25	43.842627	125.348033	75	43.915569	125.360708
26	43.805436	125.29279	76	43.77458	125.269852

Table A3. Cont.

Serial Number	Latitude/°N	Longitude /°E	Serial Number	Latitude/°N	Longitude/°E
27	43.908228	125.353404	77	43.788377	125.267272
28	43.833878	125.377279	78	43.872522	125.360277
29	43.793152	125.398239	79	43.80733	125.454246
30	43.861092	125.388539	80	43.828481	125.318853
31	43.843238	125.425431	81	43.798887	125.30516
32	43.840715	125.360151	82	43.793443	125.315005
33	43.812281	125.402488	83	43.837223	125.406287
34	43.834626	125.39462	84	43.844025	125.339175
35	43.85298	125.450993	85	43.792858	125.42437
36	43.832712	125.391496	86	43.841206	125.410059
37	43.835115	125.442014	87	43.792006	125.395835
38	43.893361	125.352221	88	43.852766	125.356367
39	43.8931	125.34364	89	43.899677	125.344485
40	43.89796	125.352507	90	43.802605	125.336546
41	43.860657	125.369726	91	43.880092	125.345643
42	43.838179	125.460384	92	43.899882	125.332816
43	43.826313	125.378839	93	43.833841	125.367847
44	43.83805	125.412816	94	43.840575	125.408217
45	43.834954	125.392255	95	43.833253	125.388789
46	43.893672	125.346473	96	43.82796	125.379248
47	43.903571	125.353122	97	43.835528	125.380312
48	43.790302	125.440001	98	43.811003	125.397103
49	43.82728	125.375988	99	43.821876	125.453335
50	43.837934	125.300282			

## References

- Yan, H.; Wu, L.; Yi, X.; Wang, D.D.; Li, X. Discussion on green express packaging. In Proceedings of the International Conference of Green Buildings and Environmental Management (GBEM), Qingdao, China, 23–25 August 2018.
- Liang, H.P.; Li, J.G. Research on the creative design of express package recycling system basis on internet. *IOP Conf. Ser. Earth Environ. Sci.* **2020**, *463*, 012089. [\[CrossRef\]](#)
- Xiao, Y.M.; Zhou, B.Y. Does the development of the delivery industry increase the production of municipal solid waste?-An empirical study of China. *Resour. Conserv. Recycl.* **2020**, *155*, 104577. [\[CrossRef\]](#)
- High, X.; Liu, C.S. Research on customers' willingness to participate in express package recycling. In Proceedings of the 5th International Conference on Energy Materials and Environment Engineering, Kuala Lumpur, Malaysia, 12–14 April 2019.
- Ding, Z.H.; Sun, J.; Wang, Y.W.; Jiang, X.H.; Liu, R.; Sun, W.B.; Mou, Y.P.; Wang, D.W.; Liu, M.Z. Research on the influence of anthropomorphic design on the consumers' express packaging recycling willingness: The moderating effect of psychological ownership. *Resour. Conserv. Recycl.* **2021**, *168*, 105269. [\[CrossRef\]](#)
- Carfi, D.; Donato, A. Plastic-pollution reduction and bio-resources preservation using green-packaging game cooperation. *Mathematics* **2022**, *10*, 4553. [\[CrossRef\]](#)
- Cheng, L.; Cao, G.R. Present situation and ideas of express packaging organization. *Adv. Graph. Commun. Media Technol.* **2017**, *417*, 697–703. [\[CrossRef\]](#)
- Yang, H.T.; Li, W.L. Construction of express packaging recovery logistics system from the perspective of ecological innovation—Take Xinyang Normal University as an example. In Proceedings of the 25th Annual International Conference on Management Science and Engineering, Frankfurt, Germany, 17–20 August 2018.
- Cai, K.H.; Xie, Y.F.; Song, Q.B.; Sheng, N.; Wen, Z.G. Identifying the status and differences between urban and rural residents' behaviors and attitudes toward express packaging waste management in Guangdong Province, China. *Sci. Total Environ.* **2021**, *797*, 148996. [\[CrossRef\]](#)
- Duan, H.B.; Song, G.H.; Qu, S.; Dong, X.B.; Xu, M. Post-consumer packaging waste from express delivery in China. *Resour. Conserv. Recycl.* **2019**, *14*, 137–143. [\[CrossRef\]](#)
- Ren, X.; Wang, Y.H. Design of express recyclable packaging bag based on green environmental packaging material. In Proceedings of the 5th International Conference on Environmental Science and Material Application (ESMA), Xi'an, China, 15–16 December 2019.
- Guo, Y.L.; Luo, G.L.; Hou, G.S. Research on the evolution of the express packaging recycling strategy, considering government subsidies and synergy benefits. *Int. J. Environ. Res. Public Health* **2021**, *18*, 1144. [\[CrossRef\]](#)
- Hua, Y.F.; Dong, F.; Goodman, J. How to leverage the role of social capital in pro-environmental behavior: A case study of residents' express waste recycling behavior in China. *J. Clean. Prod.* **2021**, *28*, 124376. [\[CrossRef\]](#)

14. Wu, S.S.; Gong, X.; Wang, Y.F.; Cao, J. Consumer cognition and management perspective on express packaging pollution. *Int. J. Environ. Res. Public Health* **2022**, *19*, 4895. [[CrossRef](#)]
15. Chen, F.Y.; Chen, H.; Yang, J.H.; Long, R.Y.; Li, W.B. Impact of regulatory focus on express packaging waste recycling behavior: The moderating role of psychological empowerment perception. *Environ. Sci. Pollut. Res.* **2019**, *26*, 8862–8874. [[CrossRef](#)] [[PubMed](#)]
16. Zheng, C.L.; Zhou, Y.Y. Multi-criteria group decision-making approach for express packaging recycling under interval-valued fuzzy information: Combining objective and subjective compatibilities. *Int. J. Fuzzy Syst.* **2022**, *24*, 1112–1130. [[CrossRef](#)]
17. Lin, G.; Chang, H.M.; Li, X.; Li, R.; Zhao, Y. Integrated environmental impacts and c-footprint reduction potential in treatment and recycling of express delivery packaging waste. *Resour. Conserv. Recycl.* **2022**, *179*, 106078. [[CrossRef](#)]
18. Harsaj, F.; Aghaeipour, Y.; Sadeghpour, M.; Rajaei, Y. A fuzzy multi-objective model for a sustainable end-of-life vehicle reverse logistic network design: Two meta-heuristic algorithms. *Int. J. Value Chain Manag.* **2022**, *13*, 47–87. [[CrossRef](#)]
19. Gao, X.H.; Cao, C.J. A novel multi-objective scenario-based optimization model for sustainable reverse logistics supply chain network redesign considering facility reconstruction. *J. Clean. Prod.* **2020**, *270*, 122405. [[CrossRef](#)]
20. Nie, D.X.; Li, H.T.; Qu, T.; Liu, Y.; Li, C.D. Optimizing supply chain configuration with low carbon emission. *J. Clean. Prod.* **2020**, *271*, 122539. [[CrossRef](#)]
21. Guo, J.Q.; Wang, X.Y.; Fan, S.Y.; Gen, M. Forward and reverse logistics network and route planning under the environment of low-carbon emissions: A case study of Shanghai fresh food e-commerce enterprises. *Comput. Ind. Eng.* **2017**, *106*, 351–360. [[CrossRef](#)]
22. Reddy, K.N.; Kumar, A.; Sarkis, J.; Tiwari, M.K. Effect of the carbon tax on reverse logistics network design. *Comput. Ind. Eng.* **2020**, *139*, 106184. [[CrossRef](#)]
23. Yang, J.H.; Long, R.Y.; Chen, H.; Sun, Q.Q. A comparative analysis of express packaging waste recycling models based on the differential game theory. *Resour. Conserv. Recycl.* **2021**, *168*, 105449. [[CrossRef](#)]
24. Wu, J.; Azarm, S. Metrics for quality assessment of a multiobjective design optimization solution set. *J. Mech. Des.* **2001**, *123*, 18–25. [[CrossRef](#)]
25. Liu, Q.G.; Liu, X.X.; Wu, J.; Li, Y.X. Multiattribute group decision-making method using a genetic K-Means clustering algorithm. *Math. Probl. Eng.* **2020**, *2020*, 8313892. [[CrossRef](#)]
26. Deb, K.; Pratap, A.; Agarwal, S.; Meyarivan, T. A fast and elitist multiobjective genetic algorithm: NSGA-II. *IEEE Trans. Evol. Comput.* **2002**, *6*, 182–197. [[CrossRef](#)]
27. Liang, X.; Chen, J.B.; Gu, X.L.; Huang, M. Improved adaptive non-dominated sorting genetic algorithm with elite strategy for solving multi-objective flexible job-shop scheduling problem. *IEEE Access* **2021**, *9*, 106352–106362. [[CrossRef](#)]
28. Pulansari, F. The analysis of cost drivers to successful implementation of reverse logistics system. In Proceedings of the 1st International Conference on Industrial and Manufacturing Engineering (ICI and ME), Medan, Indonesia, 16–17 October 2018.
29. Xu, J.G.; Qiao, Z.; Liu, J.H. Study on cost control of enterprise reverse logistics based on the analysis of cost drivers. In Proceedings of the 3rd International Conference on Wireless Communications, Networking and Mobile Computing (WiCOM 2007), Shanghai, China, 21–25 September 2007.
30. Fang, X.H.; Li, N.; Mu, H. Research progress on logistics network optimization under low carbon constraints. In Proceedings of the International Conference on Green Development and Environmental Science and Technology (ICGDE), Changsha, China, 18–20 September 2020.
31. Wang, B.; Li, H.H. Optimization of Electronic Waste Recycling Network Designing. In Proceedings of the 5th International Conference on Electromechanical Control Technology and Transportation (ICECTT), Network, Nanchang, China, 15–17 May 2020.
32. Chen, M.; Yin, C.J.; Xi, Y.P. A new clustering algorithm Partition K-means. In Proceedings of the International Conference on Advanced Materials and Computer Science, Chengdu, China, 1–2 May 2011.
33. Ge, F.H.; Luo, Y. An improved K-means algorithm based on weighted euclidean distance. In Proceedings of the 3rd International Conference on Theoretical and Mathematical Foundations of Computer (ICTMF 2012), Bali, Indonesia, 1–2 December 2012.
34. Deb, K.; Agrawal, R.B. Simulated binary crossover for continuous search space. *Complex Syst.* **1995**, *9*, 115–148.
35. Deb, K.; Goyal, M.A. Combined genetic adaptive search (GeneAS) for engineering design. *Comput. Sci. Inform.* **1996**, *26*, 30–45.
36. Vachhani, V.L.; Dabhi, V.K.; Prajapati, H.B. Survey of multi objective evolutionary algorithms. In Proceedings of the International Conference on Circuit, Power and Computing Technologies (ICCPCT), Nagercoil, India, 19–20 March 2015.
37. Osyczka, A.; Krenich, S. Evolutionary algorithms for multicriteria optimization with selecting a representative subset of Pareto optimal solutions. In Proceedings of the 1st International Conference on Evolutionary Multi-Criterion Optimization (EMO 2001), Zurich, Switzerland, 7–9 March 2001.
38. Takagi, T.; Takadama, K.; Sato, H. Supervised Multi-objective optimization algorithm using estimation. In Proceedings of the IEEE Congress on Evolutionary Computation (CEC), Padua, Italy, 18–23 July 2022.

39. Abubaker, A.; Baharum, A.; Alrefaei, M. Good solution for multi-objective optimization problem. In Proceedings of the 21st National Symposium on Mathematical Sciences (SKSM), Penang, Malaysia, 6–8 November 2013.
40. Froese, R.; Klassen, J.W.; Leung, C.K.; Loewen, T.S. The border K-means clustering algorithm for one dimensional data. In Proceedings of the IEEE International Conference on Big Data and Smart Computing (BigComp), Daegu, Republic of Korea, 17–20 January 2022.

**Disclaimer/Publisher's Note:** The statements, opinions and data contained in all publications are solely those of the individual author(s) and contributor(s) and not of MDPI and/or the editor(s). MDPI and/or the editor(s) disclaim responsibility for any injury to people or property resulting from any ideas, methods, instructions or products referred to in the content.